

***Amphicutis stygobita* (Echinodermata, Ophiuroidea, Amphilepidida, Amphilepididae), a brooding brittle star from anchialine caves in The Bahamas: feeding, reproduction, morphology, paedomorphisms and troglomorphisms**

Jerry H. Carpenter¹

¹ *Department of Biological Sciences, Northern Kentucky University, Highland Heights, Kentucky 41099, USA*

Corresponding author: Jerry H. Carpenter (carpenter@nku.edu)

Academic editor: Elizabeth Borda | Received 10 March 2025 | Accepted 26 April 2025 | Published 16 May 2025

<https://zoobank.org/B7817771-B422-44BE-9F79-6BF76A975382>

Citation: Carpenter JH (2025) *Amphicutis stygobita* (Echinodermata, Ophiuroidea, Amphilepidida, Amphilepididae), a brooding brittle star from anchialine caves in The Bahamas: feeding, reproduction, morphology, paedomorphisms and troglomorphisms. Subterranean Biology 51: 147–196. <https://doi.org/10.3897/subtbiol.51.152663>

Abstract

Amphicutis stygobita Pomory, Carpenter & Winter, 2011 was the world's first known cave brittle star. It has been found only in two anchialine caves: Bernier Cave (type locality and current study area) and Lighthouse Cave on San Salvador Island, The Bahamas. Bernier Cave's low salinity (14–28 ppt) reduces ionic precipitation in *A. stygobita*'s endoskeleton to produce fewer and lighter ossicles. Scanning electron microscopy (SEM) revealed details of internal skeletal structures including elongated arm segment ossicles with greatly reduced density and increased fenestration. The large ceiling entrance of Bernier Cave is directly above the water allowing abundant growth of algae and accumulation of detritus. Small (disk diameter = 3–4 mm) microphagous deposit-feeding brittle stars survived and grew in captivity by consuming energy-rich detritus containing algae, bacteria, invertebrates, and a sticky biofilm containing extracellular polymeric substances (EPS). Reproductive structures are described for this hermaphroditic brooding species, as are morphology and growth rates for adults and three babies born in captivity. Comparisons are made to three recently described cave species that appear to be cave endemics and to several epigean brittle stars including the brackish-water species *Ophiophragmus filograneus* and two deep-sea species: *Amphilepis patens* and *Amphilepis platytata* herein removed from synonymy. Several of these species show paedomorphy, including reduced mouth structures and arm ossicles. Paedomorphy conserves energy by not producing, maintaining, and transporting adult structures not needed for survival. Paedomorphic traits that are adaptive and occur in cave organisms are considered troglomorphic traits, as in *A. stygobita*. Correlations are made between specific paedomorphisms and environmental features.

Keywords

Amphilepis patens, *Amphilepis platytata*, detritus, energy conservation, extracellular polymeric substances, hermaphroditic, ossicles, streptospondylous

Introduction

Amphicutis stygobita, described by Pomory, Carpenter and Winter in 2011, was the world's first known cave brittle star. Pomory et al. (2011) assigned this new genus and species to the family Amphilepididae in the order Ophiurida, but this family is now placed in the order Amphilepidida, created by O'Hara et al. (2017, 2018). The small family Amphilepididae includes only the cave species *Amphicutis stygobita* and 12 species of *Amphilepis* (Stöhr et al. 2024), which are all deep sea. Caves that are close to oceans typically contain salt water or brackish water; such caves without a surface connection to the ocean are called anchialine (for definitions please see Holthuis 1973; Stock et al. 1986; Bishop et al. 2015; Carpenter 2021). *Amphicutis stygobita* has been found only in two anchialine caves: Bernier Cave (type locality) and nearby Lighthouse Cave on San Salvador Island, The Bahamas (Fig. 1A–E). It is much more abundant in Bernier Cave; to my knowledge, only two specimens have ever been found in Lighthouse Cave, and they were not used in the current study. Carpenter (2016) reported additional observations on the biology and behavior of *A. stygobita*, including apparent cave adaptations (troglomorphisms): no body pigment, reduced body size, elongated arm segments, muted alarm response to light, reduced aggregation, slow movement primarily with podia (rather than by swinging arms forward), and extremely slow regeneration of 0.03 mm/wk (this is about 1% of the average rate for 13 species reported by Clark et al. 2007). Carpenter (2016) also noted that, “They are challenging to maintain in the laboratory because they are susceptible to light, salinity changes, and elevated temperatures, and they don't accept food normally eaten by brittle stars.” The brittle stars survived and grew in captivity using cave detritus as their only food source. Comparisons are made between Bernier Cave and deep-sea environments, since the relatively high richness of detritus is presumed to be one of the main reasons the brittle star population does well in this cave and why there are so many deep-sea brittle star species.

Caves and deep-sea environments are both characterized by low food supplies because they are dark and have no primary production by photosynthesis (Culver and Phipps 2019), but this is not always the case. Bernier Cave is exceptional because the large ceiling entrance allows detritus and sunlight to enter and produce an energy-rich food source for *A. stygobita*. Similarly, some areas of the deep-sea floor are covered by abundant energy-rich phytodetritus which can provide food for brittle stars that are detritivores (Ramirez-Llodra et al. 2010). I contend that high-energy detritus promotes paedomorphy (retention of juvenile traits by adults). In both environments, the soft and sticky detritus contains extracellular polymeric substances (EPS) that provide food and may aid ingestion by brittle stars that have paedomorphically reduced mouthparts.

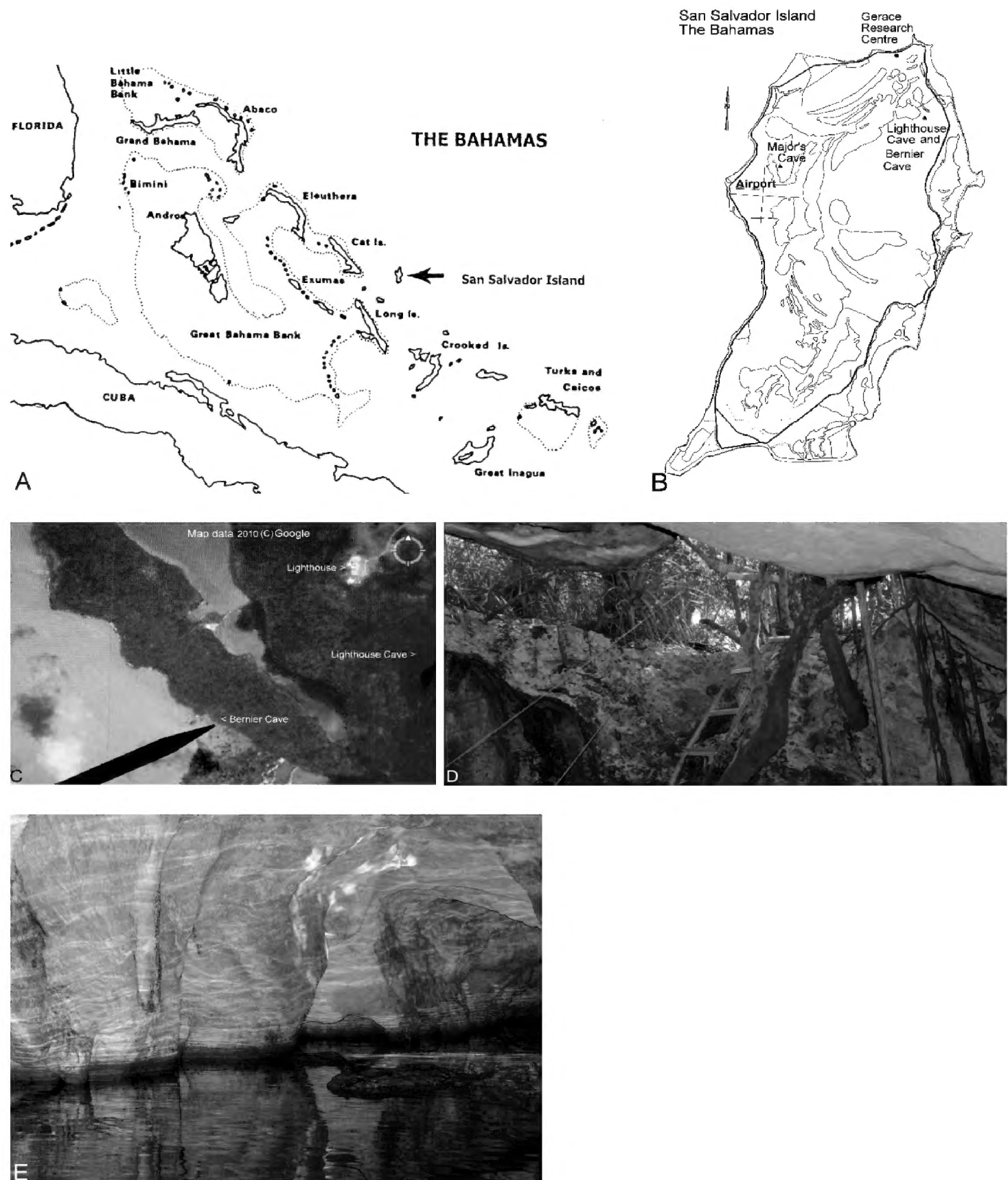


Figure 1. Location **A** map with location of San Salvador Island in The Bahamas (from Carpenter 2021) **B** map of San Salvador Island with locations of Bernier Cave and Lighthouse Cave (modified from Carpenter 2021) **C** Google earth map with location of caves **D** ceiling entrance to Bernier Cave **E** algae-covered wall below entrance to Bernier Cave.

Reproductive structures are described for this brooding species, as are morphology and growth rates for adults and three individuals born in captivity. Only about 3% (~70 species) of the 2000+ species of brittle star species are known to be brooders (Hendler 1975; Hendler et al. 1995; Stöhr 2005). Stöhr et al. (2012) indicated that there were 2064 described species of brittle stars, and “juvenile stages are still only

known for less than 50 species.” There are very few observations on the development and behavior of newly released babies, so keeping *A. stygobita* babies alive for up to 14.5 months provided valuable information.

The original description of *A. stygobita* included many detailed images using light microscopy, and it is expanded herein with descriptions of the internal skeletal structure (stereom) of adults using scanning electron microscopy (SEM). Comparisons are made to several epigean brittle star species including two deep-sea species, *Amphilepis patens* Lyman, 1879 and *Amphilepis platytata* HL Clark, 1911; although these two species were synonymized in 1917 (Clark 1917), I present evidence for them to be recognized as separate species. Comparisons are also made to the brackish-water species *Ophiophragmus filograneus* (Lyman, 1875) and to three recently described species that appear to be cave endemics: (1) *Ophiozonella cavernalis* Okanishi & Fujita, 2018 (Japan), (2) *Ophionereis commutabilis* Bribiesca-Contreras et al., 2019 (Mexico), and (3) *Ophiopsila xmasilluminans* Okanishi, Oba & Fujita, 2019 (Christmas Island, north of Australia).

Because *A. stygobita* has so many unusual traits, I felt it important to include an abundance of photographs of this species and of several species used for comparison. Hopefully, these photographs will help other researchers better understand the unusual traits. The photographs also support rare observations on feeding, birth and growth of three babies, and paedomorphic traits.

Materials and methods

Study area

Bernier Cave (24°05'37"N, 7°27'15"W) is about 1.5 km from the ocean in the north-eastern part of San Salvador Island, The Bahamas (Fig. 1A, B). The entrance is only ~20 m from the northeast arm of Great Lake (Fig. 1C). Near the cave this lake is hypersaline with salinities sometimes measuring > 70 ppt (personal observations), so it is surprising that the water inside Bernier Cave is hyposaline at ~14–28 ppt. Salinities and temperatures were measured at various locations, depths, and times in Bernier Cave using refractometers and hydrometers for salinities and a probe thermometer for temperatures. Pomory et al. (2011) noted that, “It appears meteoric water or water from a subsurface freshwater lens infiltrates Bernier Cave, so that the shallow-water environment may never reach total marine salinity of 35 ppt.” While most anchialine caves in The Bahamas and other locations around the world are stratified with a freshwater layer and halocline layer over a saltwater layer, the anchialine caves on San Salvador Island have salt water or brackish water all the way to the surface (Carpenter 2021).

One of the most important features of Bernier Cave is that the ceiling entrance is large and directly above or near the water (Fig. 1D). This allows considerable detritus to enter the aquatic ecosystem. It also provides an unusual amount of light to reach the walls of the entrance room to create abundant and colorful growth of algae (Fig. 1E), including the large dominant diatom *Campylodiscus neofastuosus* Ruck & Nakov (Ruck

et al. 2016a, 2016b) (Fig. 2A, B). The unusual brackish-water environment in Bernier Cave, along with adequate sunlight, provides an ideal habitat for *Campylodiscus* diatoms. The companion paper in this issue (Steinitz-Kannan et al. 2025) describes this diatom population from Bernier Cave and its special adaptations to thrive in low light. The detritus also contained nematodes, ostracods, harpacticoid copepods, ciliates, dinoflagellates, foraminiferans, cyanobacteria, other bacteria, and a sticky biofilm containing extracellular polymeric substances (EPS).

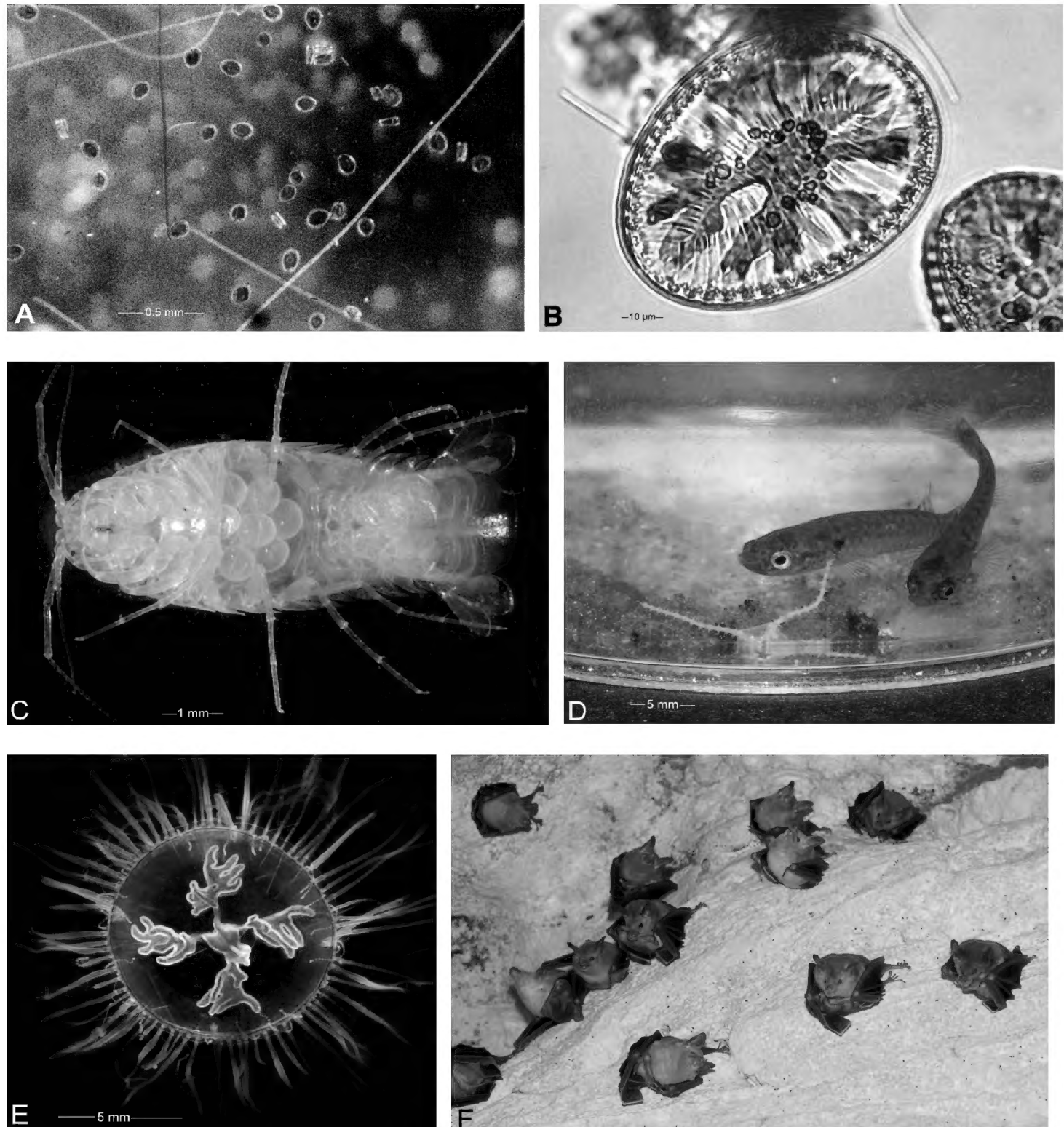


Figure 2. Large diatoms, macroinvertebrates, fish, and bats found in Bernier Cave **A** 40 × dissecting microscope view of *Campylodiscus neofastuosus* diatoms **B** compound microscope view of *C. neofastuosus* with branching chloroplast and oil droplets **C** 7.5 mm cirolanid isopod *Bahalana geracei* with ~12 eggs **D** mangrove killifish *Kryptolebias marmoratus* watching brittle star **E** 9 mm diameter hydromedusa *Vallentinia gabriellae* **F** colony of buffy flower bats *Erophylla sezekorni*, mostly females with babies, roosting in dark area of cave.

Tidal fluctuations (changes in water depth between low and high tide) are relatively slight compared to Lighthouse Cave and the ocean water surrounding the island. This results in very slow movement of water during tidal flows and allows sizeable accumulations of detritus, some of which is distributed throughout the cave with each tidal flow.

Besides *A. stygobita*, other small animals we found in Bernier Cave include the cirolanid isopod *Bahalana geracei* Carpenter, 1981 (Fig. 2C), and mangrove killifish *Kryptolebias marmoratus* (Poey, 1880) (Fig. 2D). Carpenter (2016) found that neither of these predators appeared to show interest in preying on *A. stygobita* in laboratory experiments. In 2015 my research team collected three specimens of the rare hydromedusa *Vallentinia gabriellae* Vannucci Mendes, 1848 (Fig. 2E) in Bernier Cave's entrance room; this appears to be the first record of this species in The Bahamas. Birds occasionally flew through the entrance room. Female buffy flower bats *Erophylla sezekorni* (Gundlach, 1861) with babies sometimes roosted in dark areas of the cave (Fig. 2F).

Sampling

All specimens of *A. stygobita* were found in shallow water 10–40 cm deep in dark areas of Bernier Cave using underwater flashlights. It was challenging to find specimens because this species is exceptionally small, with disk diameters (dd) of only 3–4 mm and short arms to 10 mm, and their lack of pigment helps them blend into the detritus. Our fingers and spatulas were usually used to scoot specimens into 35 mm film canisters or small clear jars; pipettes were used to transfer detritus from the substrate to small jars. Each specimen was kept in a separate container to reduce oxygen depletion and damage to arms from entangling with other specimens. They were taken to the Gerace Research Centre for short-term observation, then to Kentucky for long-term observation and experimentation. Collections were made in 2011, 2013, 2014, 2015, 2016, 2018. In most years, fewer than 6 specimens were collected, so there are insufficient numbers to warrant traditional statistical tests; however, the few specimens collected provided valuable support of observations on the biological phenomena reported herein.

Culture methods

The following culture techniques were used as reported by Carpenter (2016):

“Each specimen was kept in a small jar with ~30 ml of brackish water (20–28 ppt), similar to that of Bernier Cave. Depth in each jar was kept shallow (1–2 cm) for a high surface area to volume ratio to keep oxygen levels high. Jars had tight-fitting lids (rather than loose lids as with Petri plates) to limit evaporation that could increase salinity. Salinities were checked weekly with a refractometer. If salinity increased, it was reduced slightly by adding 1–2 ml of water at a slightly lower salinity; drops were added slowly and away from specimens to avoid salinity shock. A thin layer of detritus

from Bernier Cave was kept on the bottom of each jar to provide food and to help stabilize levels of oxygen and salinity. An additional 8–15 drops of new Bernier Cave detritus were added every 4–7 days. Animals ignored or rejected other foods offered including small pieces of TetraMin® fish flakes, shrimp, boiled egg, and boiled lettuce. Each specimen jar was labeled so individual records could be kept of maintenance, experiments, and general observations. Animals were kept in darkness except during observations and maintenance. Observations and maintenance were done at night or in a room without windows to avoid even weak sunlight, and jars were shaded from direct overhead lights and microscope lights.”

Specimens were kept near Bernier Cave temperatures of 23–25 °C (73–77 °F) by using either a 10-gallon tank with a heating pad below, or a water bath with an aquarium heater. Jars of Bernier Cave detritus were also kept in darkness at cave temperatures and salinities to try to keep them viable and to avoid temperature or salinity shock when detritus was added to specimen jars.

Photographic and SEM methods

All photos were taken by the author. Except for SEM images and one light microscope image (Fig. 4F), photographs of *A. stygobita* in this paper are of live specimens using various Nikon cameras with built-in flashes and a 60 mm micro-Nikkor lens, either shot through an Olympus dissecting microscope or directly. Photographs of some individuals were shot approximately weekly to record feeding activities, growth, and regeneration progress. The camera's built-in flash was dimmed by setting it on ½ power and using a diffuser to reduce possible disturbance or damage to specimens. Two preserved specimens were sent to Excalibur Pathology for decalcification, serial sectioning, and staining before I examined and shot photos of sections (e.g., Fig. 4F).

Several methods were used to prepare SEM specimens. Some were prepared in the traditional way of removing preserved specimens from ethanol, removing soft tissue with dilute sodium hypochlorite solution, rinsing the remaining ossicles with tap water, and mounting them on stubs. Bleaching was sometimes minimized or omitted to leave parts of specimens intact. Parts of dried museum specimens were mounted directly on stubs without bleaching. In some cases, parts of *A. stygobita* were preserved in alcohol after specimens had died and partly decomposed, and bleaching was not necessary to disarticulate ossicles. Sputter coating was not used. Northern Kentucky University's FEI Quanta 200 scanning electron microscope was used to take SEM images of more than 20 species, including *Amphilepis patens* and *Amphilepis platytata*.

Abbreviations used in text

CP - clock position; **DAP** - dorsal arm plate; **dd** - disk diameter; **DOM** - dissolved organic matter; **EPS** - extracellular polymeric substances; **LAP** - lateral arm plate; **ppt** - parts per thousand; **SEM** - scanning electron microscopy; **V** - vertebra; **VAP** - ventral arm plate.

Results

Feeding on detritus

While in Bernier Cave, the disks of *A. stygobita* took on the color of the detritus they consumed (Fig. 3A). Detritus from Bernier Cave was used successfully as food for the brittle stars in the laboratory. Before eating, adult *A. stygobita* usually had central disks that were pale yellow (Fig. 3B) and clear enough to see internal structures such as gonads (Fig. 3C, D). When a few drops of fresh detritus were added to their culture jars, they often started consuming it within minutes and their disks turned brown (Fig. 3E). They usually fed while nearly flat on the surface of the detritus, only occasionally with disk partly buried, but not with arm tips above the detritus. When new detritus was added near the edge of specimen jars, brittle stars sometimes moved to the edge and side of the jar and could be seen pulling detritus into the mouth with tube feet (Fig. 3C, D, 90 sec. apart). There seemed to be no chewing and no selection or filtering of the various light and dark components as detritus streamed into the mouth. This microphagous detritus feeding was accomplished with mouth papillae reduced in number and density, as described in the morphology section.

Reproduction, birth and growth of babies

Although gonads were not visible in preserved *A. stygobita*, in July 2018, four of the five adult *A. stygobita* that survived the 6–14 July collecting trip were each observed to contain 5–7 gonads inside their disks (Fig. 4A–D); only specimen #7 had no gonads clearly visible (Fig. 4E). The four adults with gonads (#1, 4, 5, and 6) did not appear to have gonads in their interbranchial area with a madreporite (M), which was gray and located proximal to a genital slit and near mouth structures; madreporite locations are indicated in captions for Fig. 4A–E by clock position (CP) (e.g., CP 12 is straight up, CP 6 is straight down). Most non-madreporite interbranchial areas each had 1–2 ovaries close to the genital slits near base of arms; a total of 4–5 egg-bearing ovaries appeared in most individuals; similar arrangements of gonads appeared in adults collected in previous years (e.g., Fig. 3C, D), but gonads were not counted or measured. Ovaries from the four 2018 specimens were ~0.25 to 0.75 mm in diameter, with up to 5 eggs and/or embryos visible in various stages of development, ranging in size from 0.20 to 0.35 mm. Horizontal serial sections revealed that testes and ovaries were both present in the same specimen indicating hermaphroditism (Fig. 4F).

On 17 July 2018, one adult (#5) released a baby (Fig. 5A), another emerged on 31 July, and a third appeared on 6 August. I use the term “babies” for these individuals newly released from their mother, instead of a broader term such as young or juveniles, because it better describes the specific time in their development as relatively soon after birth. Unfortunately, we don’t have a specific term for newly released brittle star babies, such as the term “mancas” used for isopods. Stöhr (2005) used the term baby in her title, “Who’s who among baby brittle stars (Echinodermata: Ophiuroidea):

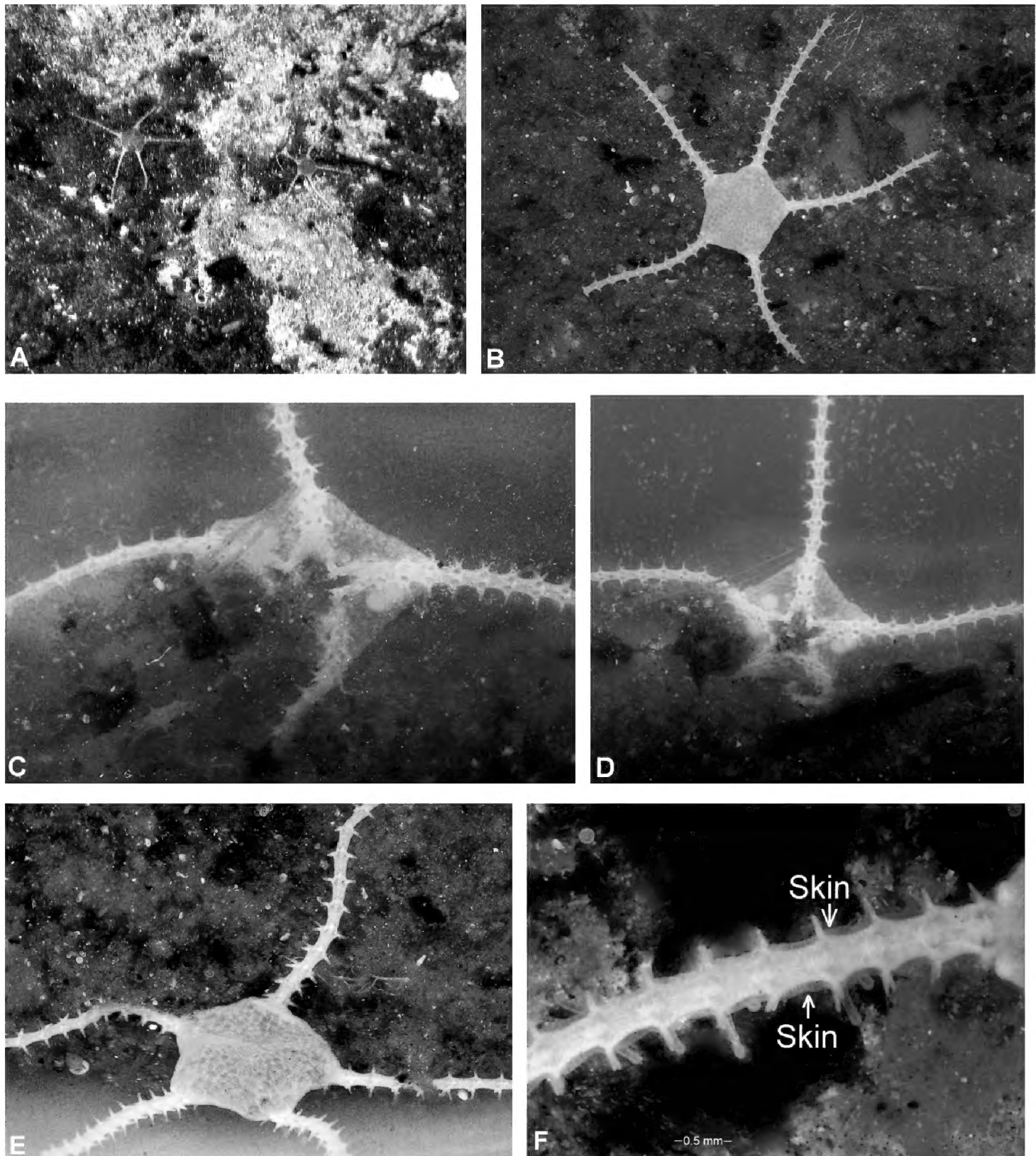


Figure 3. *Amphicutis stygobita* feeding **A** two dark adults in cave on dark substrate **B** light-colored adult before feeding **C** same animal on side of jar feeding on detritus streaming into mouth **D** same animal, 90 sec. later, with detritus in stomach **E** same animal with brown disk 25 min. after eating detritus **F** arm of adult showing skin layer.

Postmetamorphic development of some North Atlantic forms.” Stöhr (2005) noted that “the term ‘juvenile’ has been used interchangeably with ‘postlarva’ in the literature for newly metamorphosed animals to sizes of at least 2 mm disc diameter (Webb & Tyler, 1985).” Thus, the term juvenile was convenient for Stöhr (2005) and others to use for any small sexually immature individual, regardless of age. The term newborn might be appropriate for individuals shortly after being released, but it does not seem

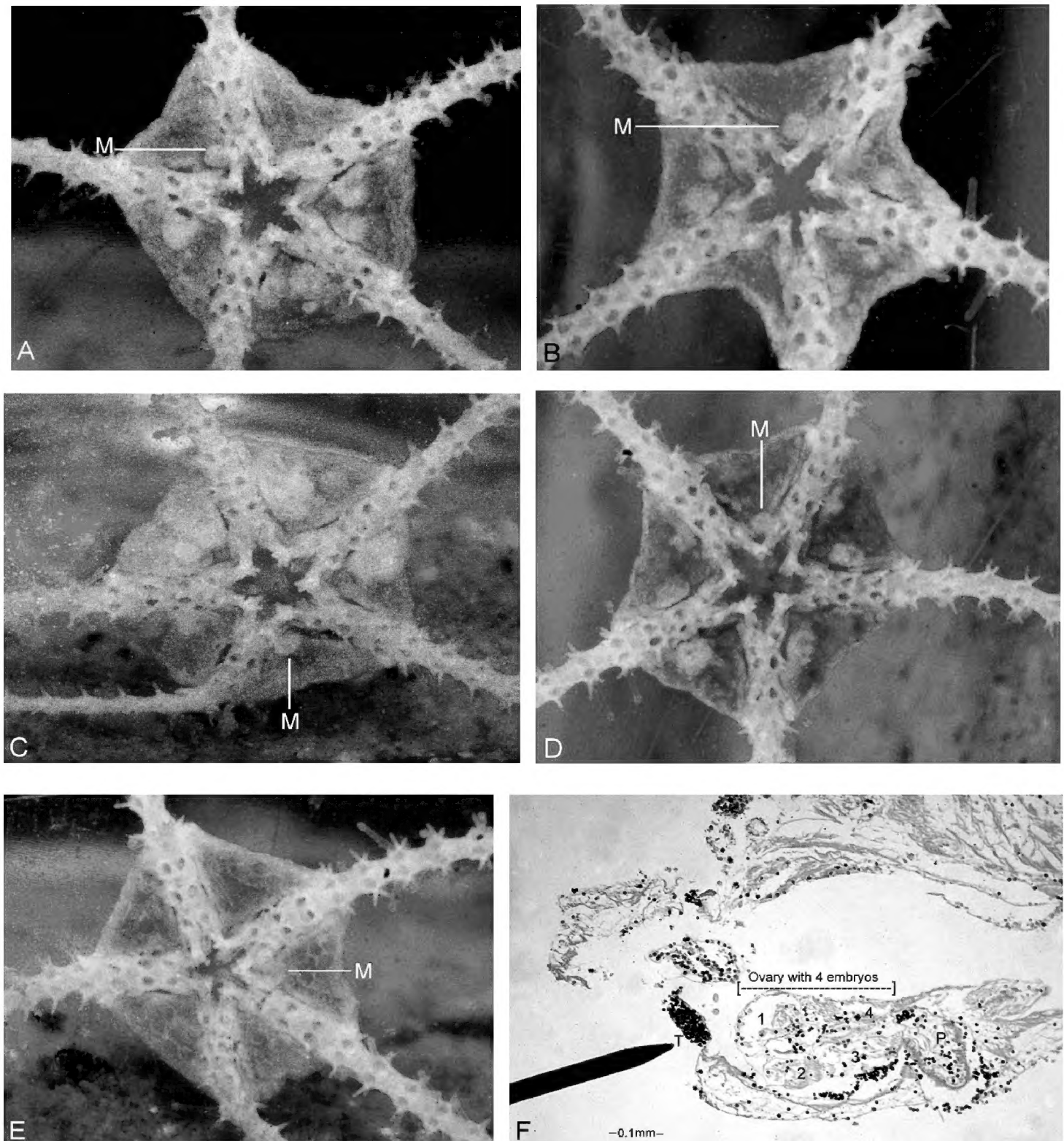


Figure 4. *Amphicutis stygobita* with gonads; all specimens with dd = 3–4 mm **A** specimen #1 with 5 gonads, madreporite (M) at clock position (CP) 11, 8 August 2018 **B** specimen #4 with 5 gonads, madreporite at CP 12, 30 July 2018 **C** specimen #5 with 5–7 gonads, madreporite at CP 6, 7 August 2018 **D** specimen #6 with 5–7 gonads, madreporite at CP 1, 30 July 2018 **E** specimen #7 with no discernible gonads, madreporite at CP 3, 24 July 2018 **F** 40 × light microscope view of horizontal section showing testis at pointer, ovary with 4 embryos (1, 2, 3, 4) near podium. Abbreviations: M – madreporite, P – podium, T – testis.

to be accurate for the same individuals after several months of growth. While some might suggest that baby seems less technical than juvenile or newborn, I contend that it is the most appropriate and accurate term for the three individuals born in this study.

Newborn babies had the following anatomical traits: disk all white (no pigment) except when brown detritus was eaten and showed through surfaces (Figs 5C, 6D);

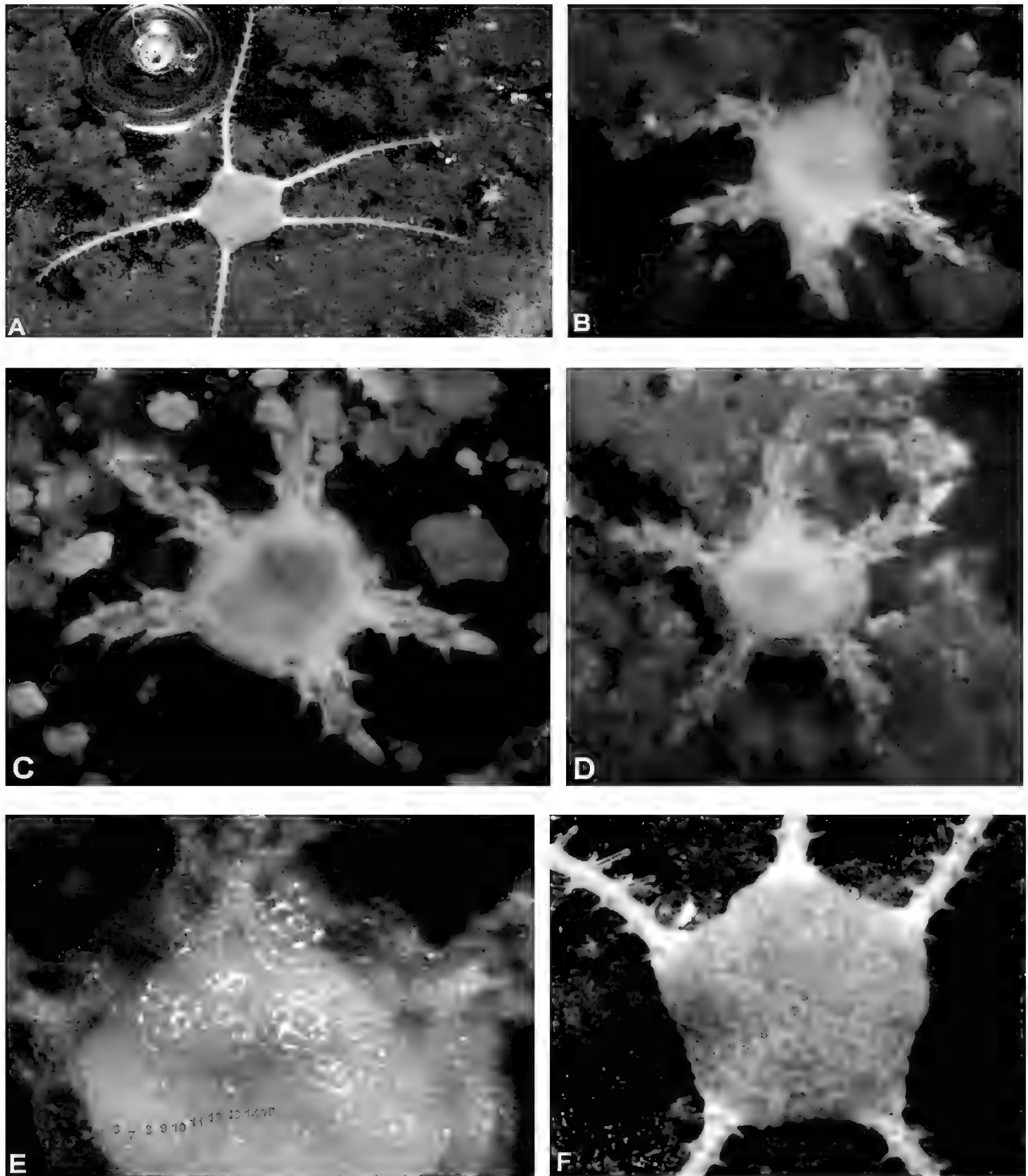


Figure 5. *Amphicutis stygobita* mother (dd = 4 mm) and babies (dd = 0.8 mm) **A** mother (adult #5) with baby #1 on right, 17 July 2028 **B** baby #1, arm at CP 4 with partially developed 3rd segment, 4 days old, 21 July 2028 **C** baby #2, food in stomach, 7 days old, 6 August 2018 **D** baby #3, clear skirt around disk, 3 days old, 8 August 2018 **E** baby #3, disk radius with ~15 scales, 8 August 2018 **F** adult #5, disk radius with ~8 scales, 17 July 2018.

disk diameter (dd) was ~0.8 mm with ~30 rows of disk scale rows (Fig. 5E), more than in adults with ~17 rows (Fig. 5F); skirt of skin with disk scales surrounded the white central disk (Fig. 5B–E); disk rounded at first (Fig. 5B–D) and became more pentagonal in a few weeks (Fig. 6C–F). Possible central and radial primary plates were visible in some images of baby #3's disk (Figs 5D–E, 6A), but if they were actually present, they

were often obscured by disk scales. Only 1 arm segment was within disk (Fig. 6F). All three babies had only 2 segments per arm beyond disk, except for baby #1 that had the beginning of a third segment on 1 arm (Fig. 5B). Each arm segment was ~ 0.2 mm long, then a cream-colored terminal plate ~ 0.2 mm long with a groove at the end bearing a short clear terminal tube foot ~ 0.04 mm long (Figs 5B, 6A–C); each arm was ~ 0.6 mm long; arm segments were flared at distal ends to accommodate podia, podian basins, and spines (Figs 5B, 6A–F); arm segments near disk were covered by small scales similar to those on disk (Figs 5B–D, 6A–C). Lateral arm plates (LAPs) were well developed to support the 2 arm segments, with each LAP bearing 2 distal spines (Figs 5B–D, 6B); dorsal arm plates (DAPs) appeared to be absent, although tiny white structures visible between segments 1–2 could have been either DAPs or part of the vertebral joints (Fig. 5C, D); good ventral views of babies were not available in their first few months, but VAPs were clearly visible when baby #2 was 8.5 months old (Fig. 6F). Developing vertebrae (Vs) were visible inside the 2 arm segments; the most apparent vertebral structures were the 2 parallel ambulacral plates that form support for adjoining parts (Figs 5B–D, 6B–F).

The behaviors of all 3 babies were similar, except that baby #1 hardly moved for several days; the other two were moderately active from near birth. They all started eating detritus within a few days of birth (Fig. 5C); detritus continued to be their only food source for as long as they lived, which was up to 14.5 months. They reacted negatively to the weak lights used to observe them (otherwise, they were in total darkness); they moved away from the light and sometimes hid under or behind detritus to stay out of direct light. Each baby was often found in the same area of its jar several days in a row, indicating they didn't move much in the dark. Arms were too short to effectively move babies forward by swinging arms, so they glided slowly on their podia (podial walking); however, they did move arms from side to side, especially the distal segment and terminal plate (Figs 5B, 6A, B). All three babies grew very slowly. The beginning of third segments could be seen developing within 2–4 months of birth (Fig. 6B). Lateral arm plates appeared to be the first arm ossicles to form in new segments, followed by VAPs and Vs (Fig. 6F). Baby #2 lived the longest (from 31 July 2018 to 14 Oct. 2019 = 14.5 months). Its dd increased from ~ 0.80 to 0.85 mm, arm length increased from ~ 0.6 to ~ 0.8 mm, and three arms each added a third segment with distal spines (Fig. 6E); third segments were ~ 0.2 mm long when distal spines developed, but they were narrower than the first two segments (Fig. 6E, F).

Morphology of adult *Amphicutis stygobita*

John Winter collected the first specimens of brittle stars from newly discovered Bernier Cave in 2009, which he sent to me. I was struck by their lack of color, very small size, and arm segments that were proportionately longer (L:W ~ 1.5) than those of all the other 13 genera illustrated in a key (Pomory 2007). These unusual traits were confirmed by Pomory et al. (2011) and are still worth emphasizing. When Pomory et al. (2011) described *Amphicutis stygobita* as a new genus and species, SEM images were not available for the description, but they now supplement the original description and confirm some of its unusual traits.

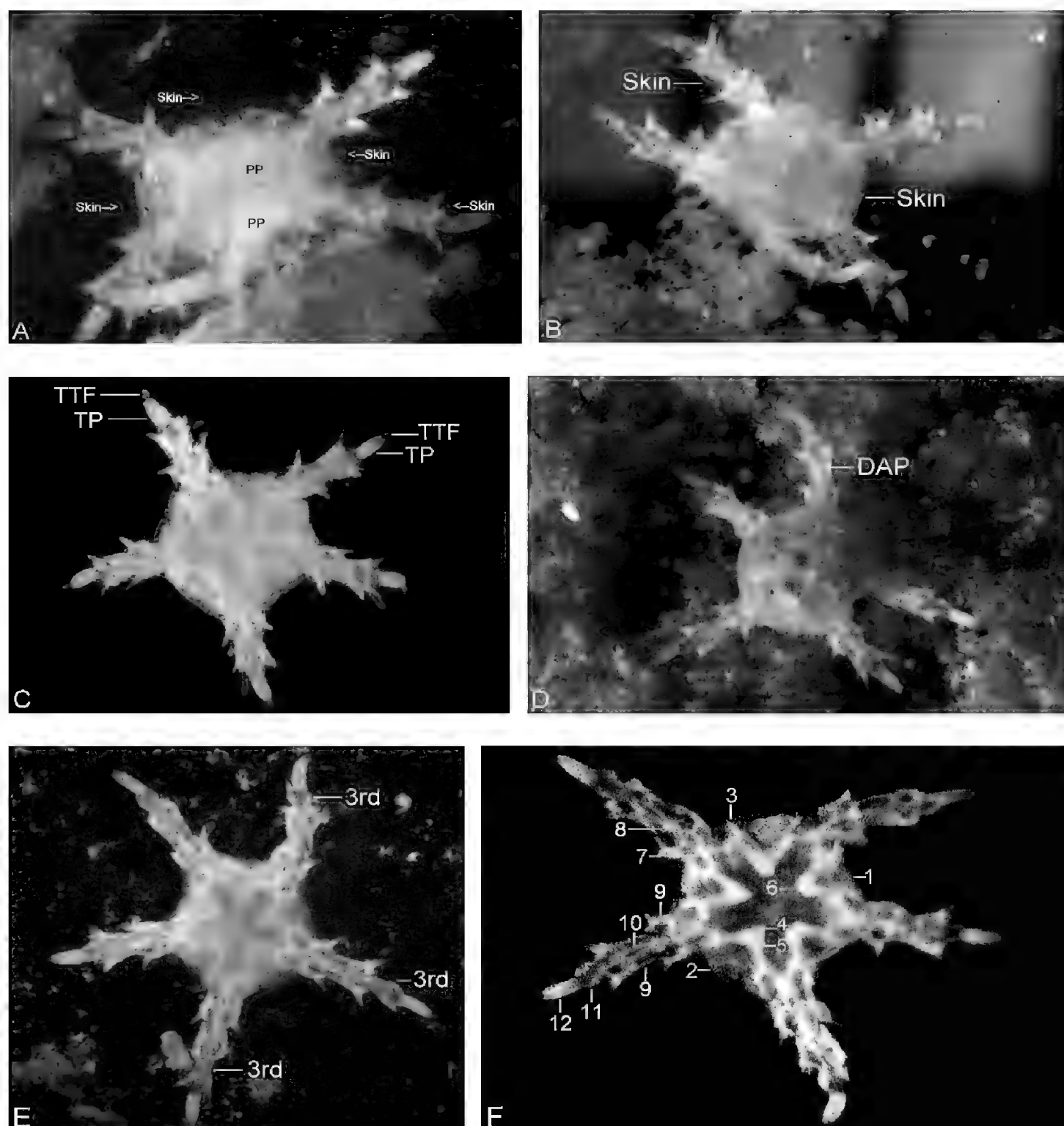


Figure 6. *Amphicutis stygobita* development, all dorsal (aboral) except 6F **A** baby #3 with skin and possible primary plates, 19 September 2018 **B** baby #3, skin on disk and arm, 31 December 2018 **C** baby #2, disk pentagonal, arms with grooved terminal plate and terminal tube foot, 30 October 2018 **D** baby #2 full of detritus, probable DAP, 29 December 2018 **E** baby #2, 13.5 months old, some arms have 3rd arm segments with 1-2 terminal spines, 14 September 2019 **F** baby #2 ventral (oral) surface showing parts of stereom, 9 April 2019: 1 madreporite, 2 disk scales, 3 adoral shield spine, 4 ventral tooth, 5 dental plate, 6 oral tentacle, 7 VAP #1, 8 VAP #2, 9 LAP, 10 ambulacral plate, 11 3rd segment outside disk, 12 terminal plate. Abbreviations: DAP – dorsal arm plate, PP – primary plates, TP – terminal plate, TTF – terminal tube foot.

The dorsal side of the disk of *A. stygobita* is covered by highly fenestrated scales (Fig. 7A, B). SEMs of the ventral disk (Figs 8A–C, 9) show the extreme variability of ossicles that was expressed by Pomory et al. (2011), “except for the distal large papillae, no two jaws have the same papillae arrangement” and “many missing due partly to

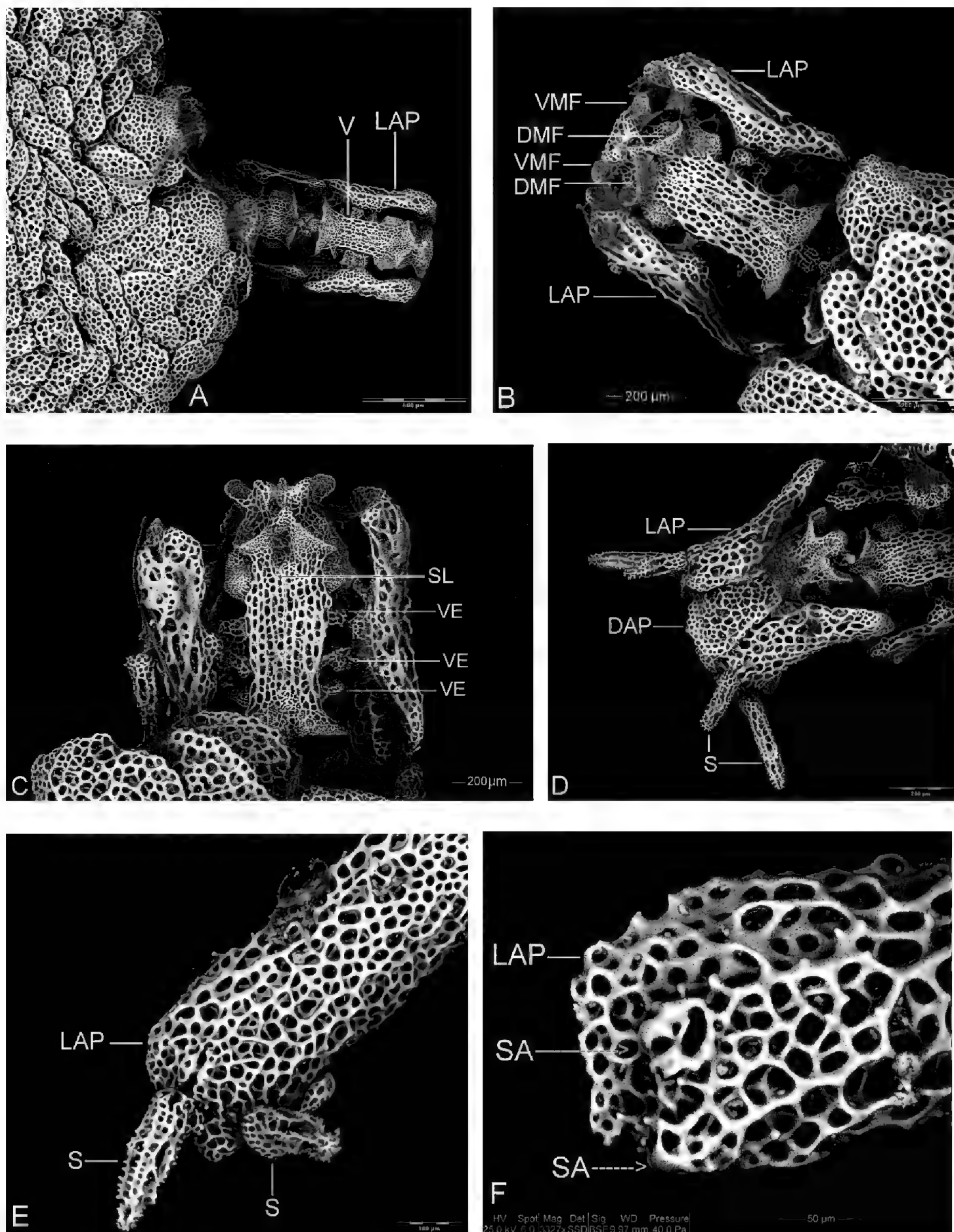


Figure 7. *Amphicutis stygobita* dorsal (aboral) SEMs **A** disk with fenestrated scales, 1st 2 arm segments, Vs with lateral extensions **B** 1st arm segment, ventral muscle flange extends past dorsal muscle flange **C** 1st arm segment, middle of LAPs curve inward to meet 3-4 vertebral extensions **D** 1st arm segment, dorsal arm plate, LAP with 2 spines **E** LAP with 2 fenestrated spines **F** LAP with 2 spine articulations. Abbreviations: DAP – dorsal arm plate, DMF – dorsal muscle flange, LAP – lateral arm plate, PB – podian basin, S – spine, SA – spine articulation, SL – suture line, V – vertebra, VAP – ventral arm plate, VE – vertebral extension, VMF - ventral muscle flange.

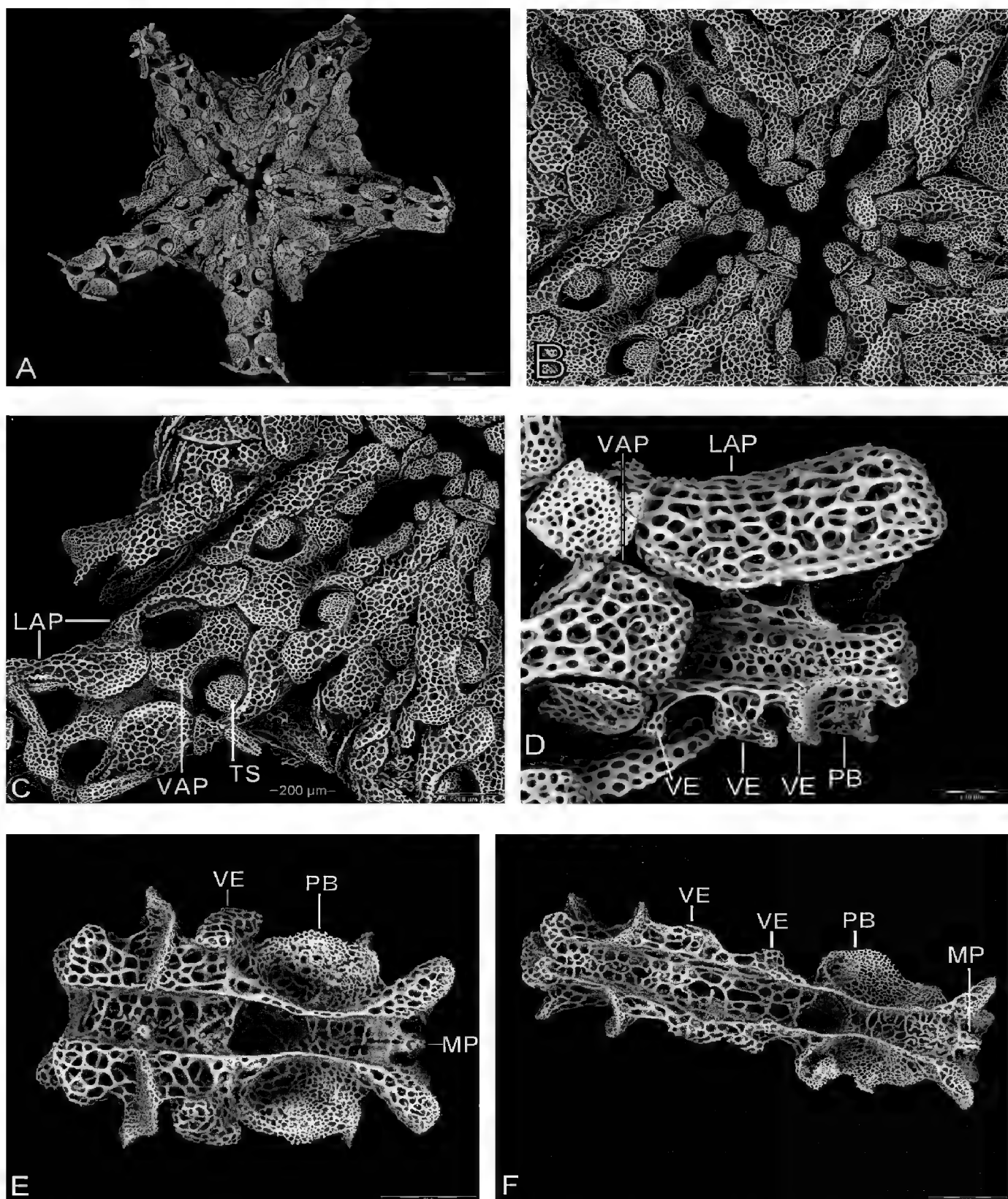


Figure 8. *Amphicutis stygobita* ventral SEMs **A** disk and 1 or 2 segments of each arm distal to disk, 1 complete segment within disk but outside mouth slit at CP6 and CP 8, 1.5–2 segments within disk at CP 11, CP 1, and CP 3 **B** oral frame showing mouth structures (see Fig 9 for labelled structures) **C** base of arm at CP8 from Fig 8A, 1 complete segment within disk with LAPs, tentacle scales, and VAPs, interbranchial areas with scales **D** 1st segment beyond disk with LAP, V with lateral extensions **E** V from proximal area of arm, large podian basin, distal to right, length $1.4 \times$ width **F** V from mid-section of arm, distal to right, length $\sim 3 \times$ width. Abbreviations as in Fig. 7 plus TS - tentacle scale.

uncalcified state.” This uncalcified state relates to the extreme fenestration of ossicles seen in SEMs (Figs 7–11). Several other key morphological traits are associated with the oral frame, including: ventral tooth shape, oral plates, oral shields, location of 2nd

tentacle pore, and number of arm segments within disk. Most of these oral frame features can be seen in SEM images (Figs 8A–C, 9); their significance is covered in the Discussion of Adult Morphology.

The ossicles of brittle star arm segments consist of a central vertebra (V) enclosed by a dorsal arm plate (DAP), a ventral arm plate (VAP), and 2 lateral arm plates (LAPs) (one on each side) (Fig. 10D). One of the most extraordinary features of *A. stygobita* is the arrangement of arm segment ossicles, with reduced DAPs and VAPs, and elongated LAPs (Figs 7A–D, 8B, C) that run parallel to Vs and connect directly to them. This is in contrast to most brittle stars that have LAPs that extend laterally from the vertebral plane. The arm ossicles of *A. stygobita* are also unusual because they are highly fenestrated with a net-like lattice of bones (trabeculae) around large open spaces where soft tissue (stroma) was before SEM preparation, similar to those seen in disk ossicles. Tentacle pores are relatively large with one large tentacle scale on the lateral side (Fig. 8A–C). Two spines are located near the distal end of LAPs (Figs 7D, E, 10D). Arm spine articulations are nearly round with 2–3 openings for muscles and nerves to pass through to the spine (Fig. 7F).

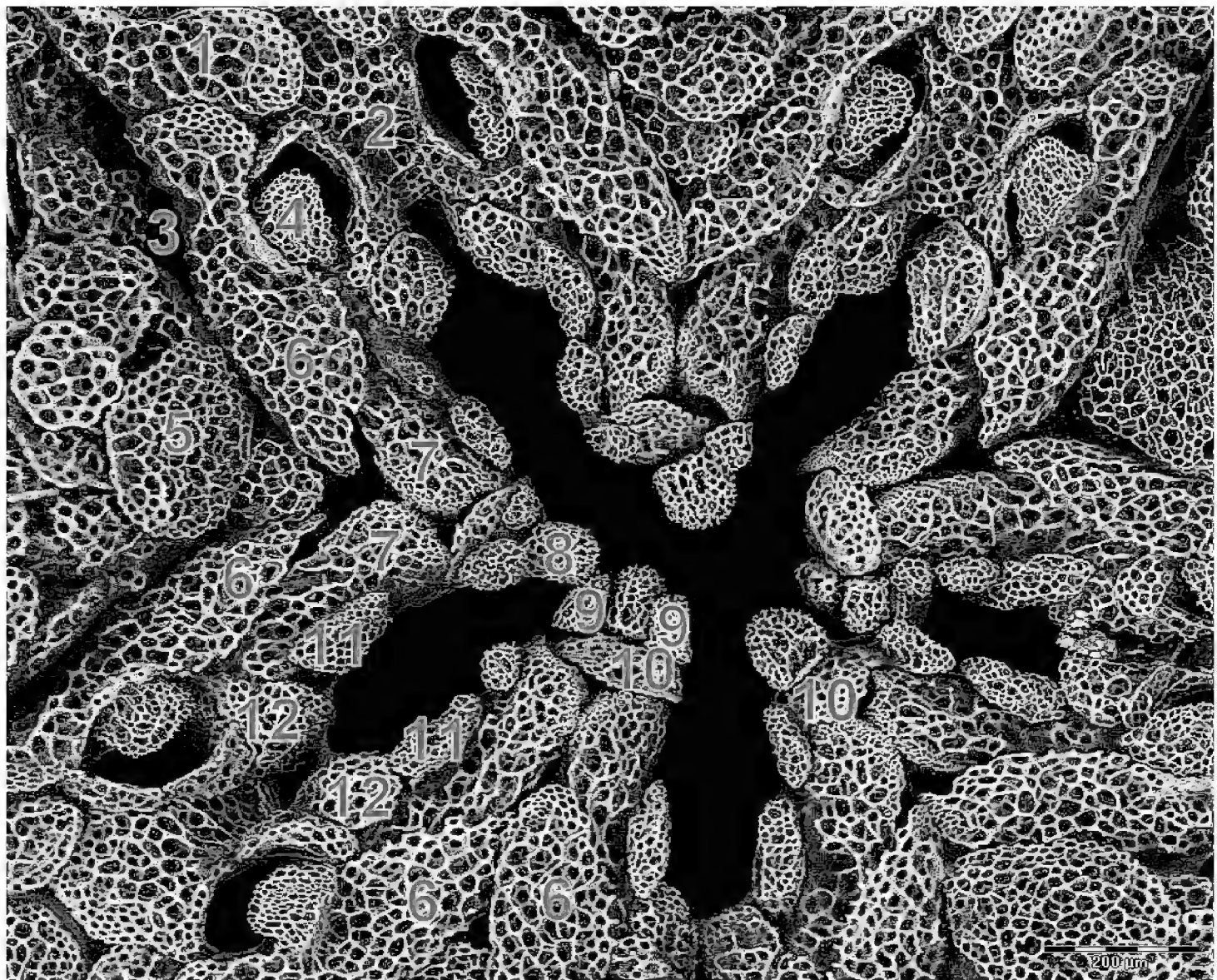


Figure 9. *Amphicutis stygobita* ventral SEM, oral frame enlargement of Fig. 8B. Numbers: 1 - 1st lateral arm plate, 2 - 1st ventral arm plate, 3 - genital slit, 4 - 2nd tentacle scale, 5 - oral shield, 6 - adoral shields, 7 - oral plates, 8 - ventral tooth, 9 - infradental papillae, 10 - dental plate, 11 - 2nd oral papillae, 12 - distal oral papillae.

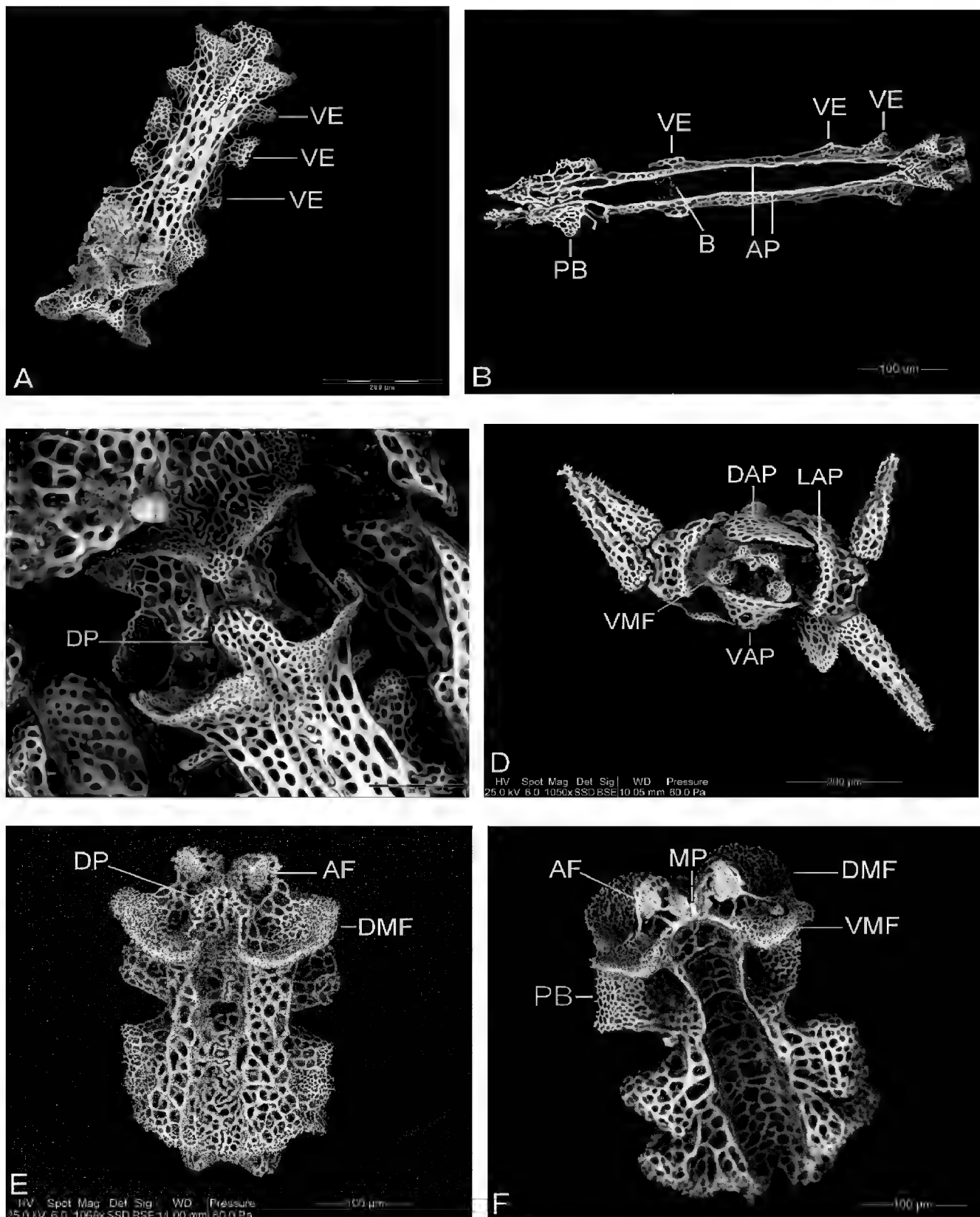
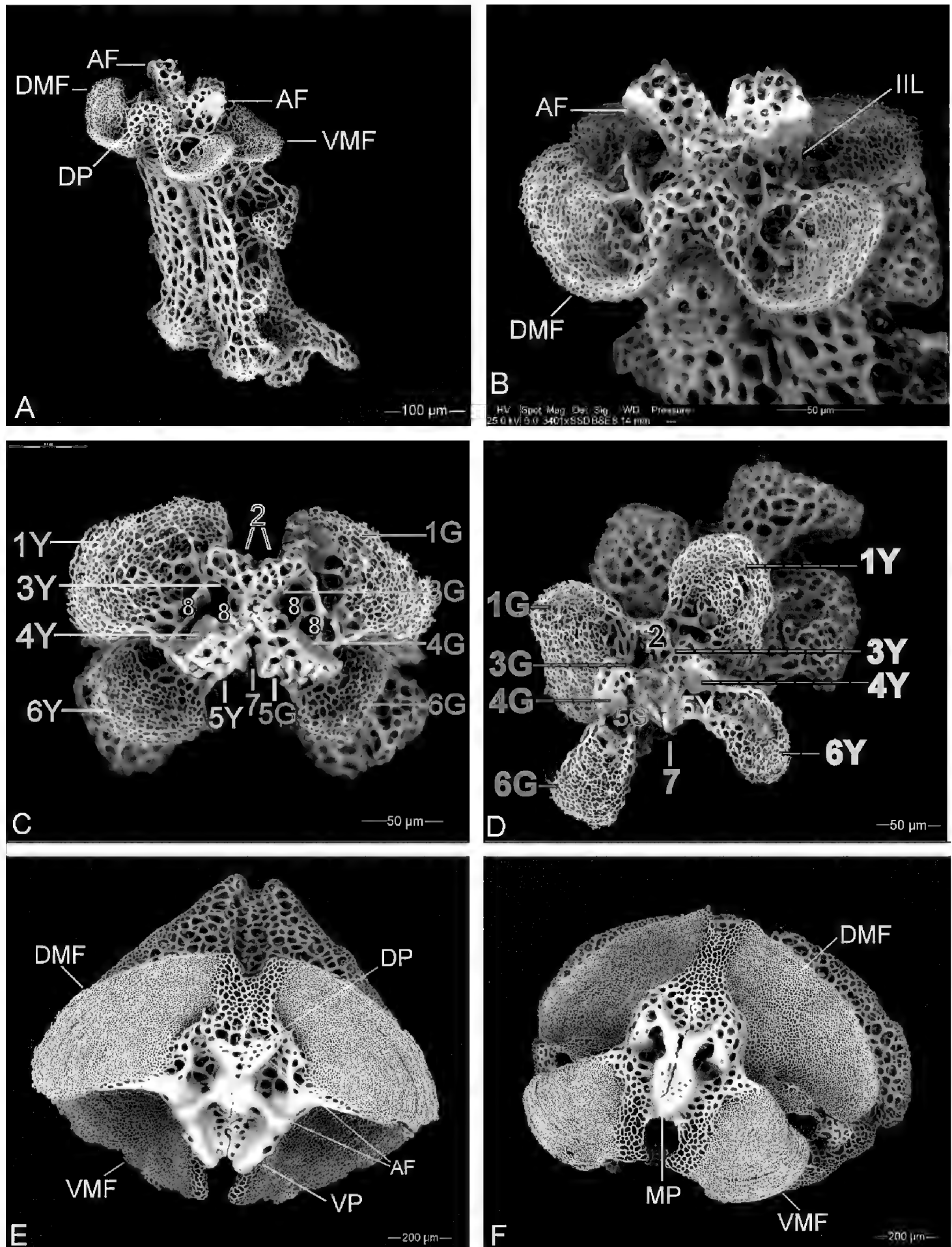


Figure 10. *Amphicutis stygobita* SEMs of vertebrae (Vs) **A** V from mid-section of arm with lateral extensions, length $\sim 3 \times$ width, dorsal view, distal down **B** V from distal area of arm, length $\sim 6 \times$ width, ventral view, distal left, bridge formed between ambulacrals **C** joint between 1st 2 Vs outside disk, dorsal, distal down **D** distal face of segment showing V enclosed by DAP, VAP, and 2 LAPs with spines **E** dorsal/proximal end view of V tilted ~ 40 degrees showing proximal end (up) with large dorsal muscle flanges and 2 articulating facets (top) **F** ventral view of V rotated to show distal end with dorsal and ventral muscle flanges, 2 articulating facets, and median process. Abbreviations as in Fig. 7 plus: AF- articulating facet, DP – dorsal process, MP – median process.

Since Pomory et al. (2011) did not have access to SEM, our description emphasized external structures, and vertebrae were little mentioned. Some unusual features of the Vs were revealed by SEMs. Arm segments of brittle stars are often shortest near

the disk and are elongated distally where new segments are produced, so it is useful to indicate location of segments and Vs in SEM images. Figs 7A–D, 8D, and 10C are from *A. stygobita* segments near disk; Figs 8E, F, 10A, E, F are Vs from near the middle of arms; Fig. 10B is a very narrow V from the distal end of arm with a thin bridge formed between the 2 central ambulacral plates.



Length of Vs varies with location on arm, but in most species the length is seldom more than twice the width. However, Vs of *A. stygobita* are about 2 to 8 times longer than wide (narrowest near distal ends of arms) (Fig. 10B). Lateral extensions of Vs connect with LAPs; Vs near disk have 3–4 narrow extensions on each side, most of which connect to protrusions near the middle of LAPs (Figs 7A–C, 8D). Lateral extensions on some Vs are flared or knobbed to form wider attachment points to LAPs (Figs 8D, 10A, E), and some lateral extensions form interrupted ridges for attachment points (Figs 8E, 10F). A pair of large podian basins near distal ends of oral surfaces of each V serve as bases for podia (Figs 8E, F, 10F). These large podian basins with their accompanying podia result in flared distal ends of segments (Figs 5A, 7A, 8A). LAPs twist around lateral sides of podia, and hourglass-shaped VAPs curve around the medial sides of podia (Fig. 8A–C). A suture line is visible along the middle of each V on both the dorsal and ventral surfaces (Figs 7A–C, 8D–F, 10A). Sutures result from the joining of the 2 ambulacral plates that are prominent in newly generated Vs in adults (Fig. 10B) and are detectable in babies (Fig. 6B–F).

The distal ends of Vs near disk have dorsal muscle flanges (= aboral muscle areas, or fossae) that are more proximal than ventral flanges and are arrow-shaped (Figs 7A–C, 10A) with arrow tips forming part of dorsal articulating projections (= dorsal processes) (Figs 8E, F, 10E, 11C). The ventral muscle flanges on distal ends of Vs extend more distally than dorsal muscle flanges (Figs 7A–C, 10A, F) with the ventral processes extending furthest (Figs 7C, 8E, F). The proximal ends of Vs near disk have dorsal muscle flanges with faces that appear to be perpendicular to the vertebral axis in dorsal view (Figs 7A–C, 10A), but they actually curve proximally and ventrally (Figs 7D, 10C, E,

Figure 11. SEMs of vertebrae ends, *Amphicutis stygobita* **A–D**, *Amphilepis patens* **E–F**. **A** dorsal/side view, proximal end up showing muscle flanges, articulating facets (top) and proximal extension of center of dorsal muscle flanges (upper left) to form dorsal process that supports dorsal articulating facets (on opposite side, out of view) **B** tilted proximal end showing dorsal muscle flanges in front, 2 ventral articulating facets behind, insertion point for intervertebral ligaments, dorsal view **C** proximal face showing: 1Y (yellow) left dorsal muscle flange, 1G (green) right dorsal muscle flange, 2 (black) dorsal process, 3Y (yellow) left dorsal articulating facet, 3G (green) right dorsal articulating facet, 4Y (yellow) left ventral articulating facet, 4G (green) right ventral articulating facet, 5Y (yellow) left side of ventral process, 5G (green) right side of ventral process, 6Y (yellow) left ventral muscle flange, 6G (green) right ventral muscle flange, 7 (red) median socket, 8 (white) insertion points for intervertebral ligaments **D** distal face showing: 1G (green) right dorsal muscle flange, 1Y (yellow) left dorsal muscle flange, 2 median depression, 3G (green) right dorsal articulating facet, 3Y (yellow) left dorsal articulating facet, 4G (green) right ventral articulating facet, 4Y (yellow) left ventral articulating facet, 5G (green) right side of ventral depression, 5Y (yellow) left side of ventral depression, 6G (green) right ventral muscle flange, 6Y (yellow) left ventral muscle flange, 7 (red) median process. (If image **D** is turned over face down to left to meet image **C**, green structures connect with corresponding green structures, yellow with yellow, red with red, and black with black), **E** proximal face of *Amphilepis patens* vertebra, large dorsal muscle flanges with growth rings, thick dorsal and ventral processes with articulating facets, **F** distal face of *A. patens* vertebra, large dorsal and ventral muscle flanges with growth rings, thick rounded tongue-shaped median process. Abbreviations as in Fig. 7 plus: IIL – insertion for intervertebral ligaments, MP – median process, VP – ventral process.

11A, B). Vertebrae are very narrow so their ends are greatly reduced in surface area, and the projections and depressions that fit into the complimentary articulating surfaces of adjacent ossicles are highly modified (Figs 10E, F, 11A–D). Ventral processes extend beyond muscle flanges and contain the ventral articulating facets; these processes appear as posts in Fig. 11A. The median process (on distal end view, Fig. 11D) is thin and wedge shaped; it fits into the corresponding median socket (on proximal end view, Fig. 11C). The complex arrangement of these vertebral projections and depressions can be better visualized by imagining the connections resulting if Fig. 11D is turned over face down to meet Fig. 11C; then the green structures would connect with corresponding green structures, yellow with yellow, red with red, and black with black. The strong fenestration appearing in other body parts of *A. stygobita* are also prominent in the ends of Vs, including muscle flanges and the post-like processes holding dorsal and ventral articulating facets (Figs 10E, F, 11A–D). Insertion points for intervertebral ligaments are trabeculae located between dorsal muscle flanges and the dorsal process (8's in Fig. 11C) and are reduced in size and number compared to other species such as *Amphilepis patens* (Fig. 11E).

Morphology of *Amphilepis patens* and *Amphilepis platytata*

Amphilepis patens Lyman, 1879 (Figs 11E, F, 12A–F, 13A–F) and *Amphilepis platytata* HL Clark, 1911 (Figs 14A–F, 15A–F) were selected for comparisons to *A. stygobita* because they are in the family Amphilepididae, as is *A. stygobita*, according to O'Hara et al. (2018). In the original description of *A. stygobita*, Pomory et. al. (2011) compared the new genus *Amphicutis* to *Amphilepis*, the only other genus in the family Amphilepididae, with 12 species of *Amphilepis* considered valid (Stöhr et al. 2024).

Gordon Hendler kindly sent me four *Amphilepis* specimens from the Natural History Museum of Los Angeles County: two (10–12 mm dd) were labelled “*Amphilepis patens* Lyman, 1879, 26 OCT 1989” (Fig. 12A, B); two (both ~9.0 mm dd) were labelled “*Amphilepis platytata* HL Clark, 1911, 2 MAR 1992” (Fig. 14A, B). My SEMs of these specimens showed several distinct differences, so it is interesting to note that *Amphilepis platytata* was synonymized with *Amphilepis patens* by HL Clark (1917); apparently this was not widely known or recognized until reported relatively recently in the World Ophiuroidea Databases by Stöhr et al. (e.g., 2024 and earlier). Clark (1917), while examining 550 specimens from deep-sea samples (to 2235 fathoms = 4087 m), made his decision on synonymy because 2 small specimens “6.5–8 mm dd” had traits of *A. platytata* (“no tentacle scales and the interbrachial areas below are perfectly naked”), while 8 others (10–12.5 mm dd, and apparently from different locations) had traits of *A. patens* (“interbrachial areas below are fully covered with scales”); he concluded that the morphological differences were probably due to “growth-stages and at any rate a matter of individual diversity.” Based on my SEM specimens, it is my opinion that Clark (1917) should not have synonymized *A. platytata* with *A. patens*, and I consider them to be separate species in this paper. Hopefully, other researchers will examine additional specimens to confirm this.

LACM 1989-147.24
 Ophiuroidea Amphilepididae
Amphilepis patens
 Lyman, 1879
 ca. 230 km W of Pt. Arguello, Santa Barbara Co.,
 California
 34° 48' N, 123° 0' W
 Coll: K.L. Smith, R/V NEW HORIZON
 Sta: NH 216M Cr: PULSE 2
 Depth: 4100 m Date: 26 OCT 1989
 Hab/Gear: otter trawl
 Pres: ETOH
 ID: C. Groves Ex: SIO
 NATURAL HISTORY MUSEUM OF LOS ANGELES COUNTY

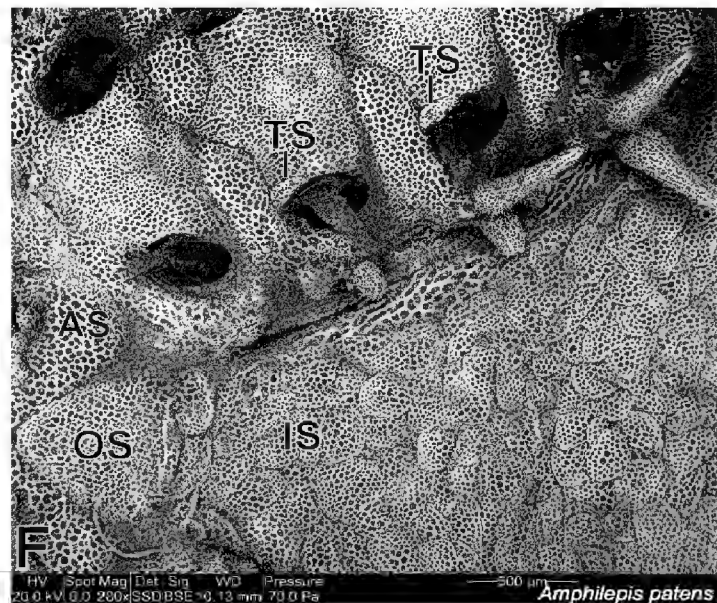
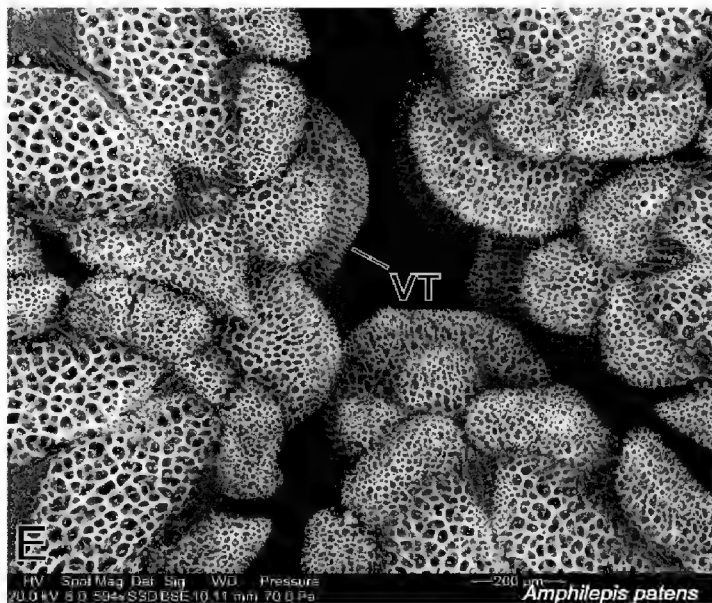
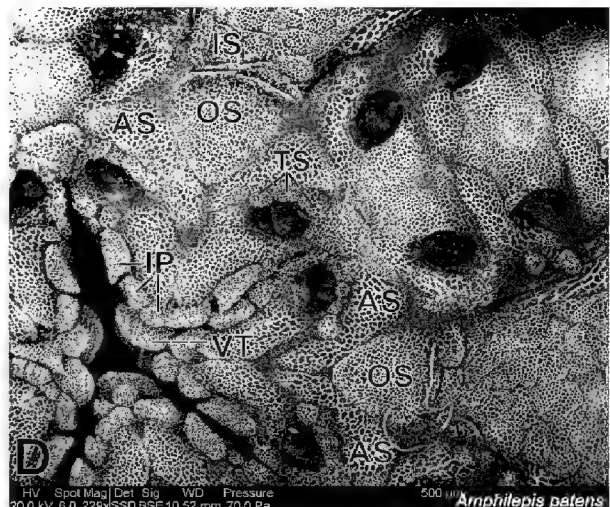
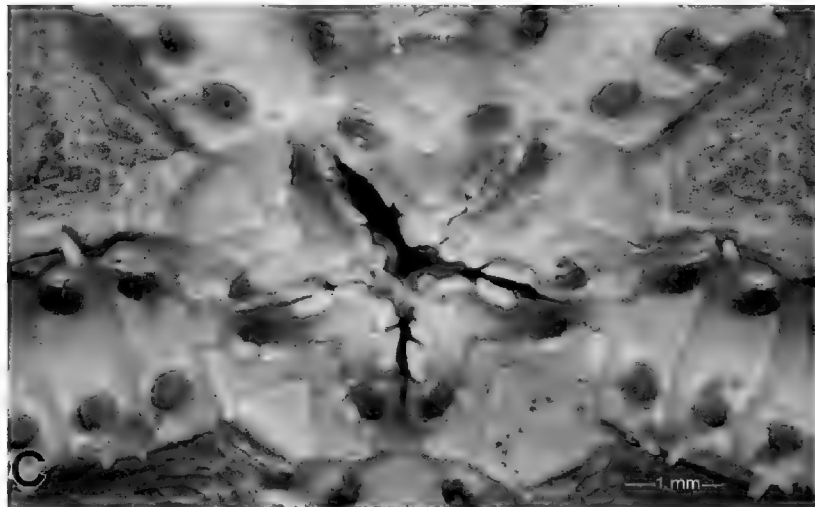
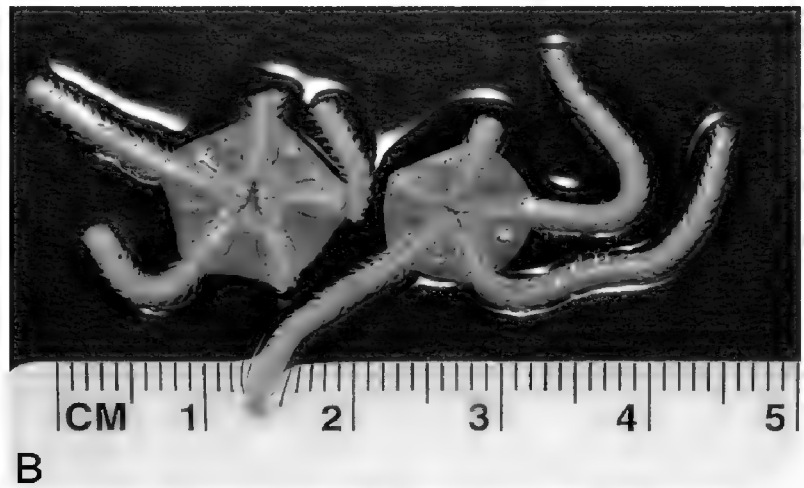


Figure 12. *Amphilepis patens* **A** museum label **B** ventral view of two preserved specimens, arms with many short segments, 4-5 arm segments within disk **C** mouth area before SEM preparation **D** SEM of mouth area and disk arm segments lightly bleached, triangular oral shields, interbrachial scales, rounded ventral teeth, elongated infradental papillae, 3 scales on oral tentacle pores **E** SEM of mouth area with rounded ventral teeth, elongated infradental papillae **F** SEM of disk arm segments with small tentacle pore scales, triangular oral shield, interbrachial scales. Abbreviations: AS – adoral shields, IP – infradental papillae, IS – interbrachial scales, OS – oral shields, TS – tentacle scales, VT – ventral teeth.

Here are three important differences I noticed on my SEMs of these two species, along with comments from the original descriptions. (1) *A. patens* has 3-4 tentacle scales adjacent to adoral shields near mouth slit (Fig. 12C–E), 1 small tentacle scale on lateral side of some VAPs distal to adoral shields (Fig. 12F) (Lyman 1879: “one minute

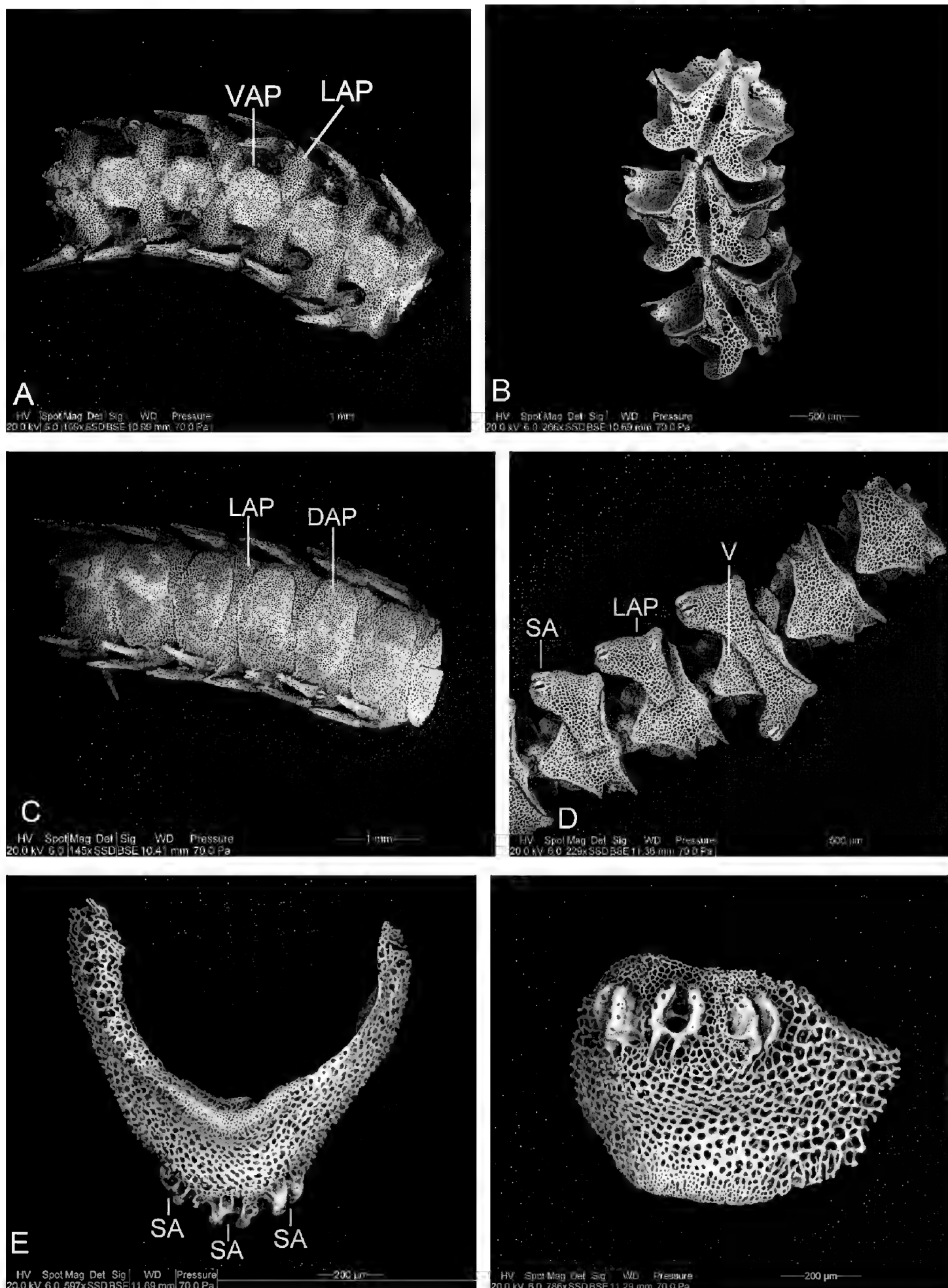


Figure 13. SEMs of *Amphilepis patens* **A** ventral view of 5 segments partially bleached, VAPs hexagonal, large LAPs with spines **B** ventral view of 3 bleached Vs **C** dorsal view of 6 wide arm segments partially bleached, LAPs between DAPs **D** dorsal view of 5 partially bleached Vs, 3 LAPs with 2 spine articulations visible, LPs attached atop Vs **E** LAP side view of 3 spine articulations **F** LAP dorsal view of 3 spine articulations. Abbreviations as in Fig. 12.

LACM 1992-233.5
 Ophiuroidea Amphilepididae
Amphilepis platytata
 H.L. Clark, 1911
 Off Big Sur coast, Monterey Co., California
 36° 26.53' N, 122° 30.71' W
 Coll: R/V POINT SUR
 Sta: M-7 Cr:
 Depth: 2810-2900 m Date: 2 MAR 1992
 Hab/Gear: beam trawl
 Pres: ETOH
 ID: Ex: MLML
 A NATURAL HISTORY MUSEUM OF LOS ANGELES COUNTY

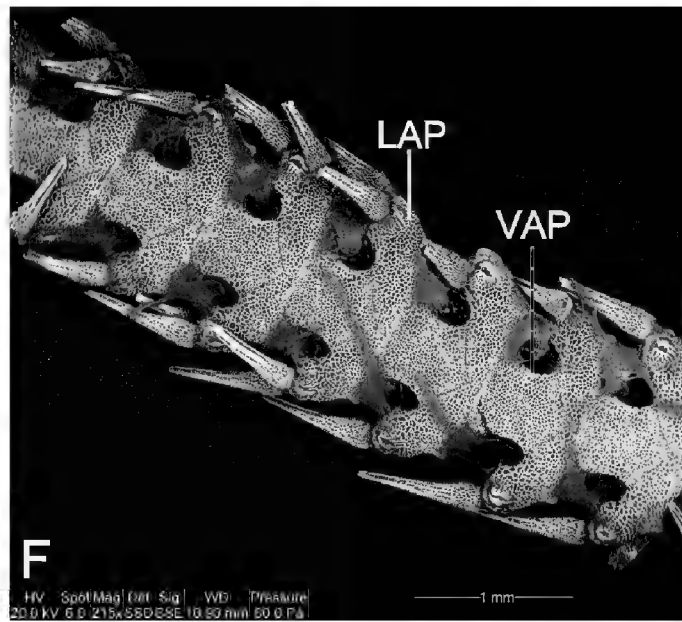
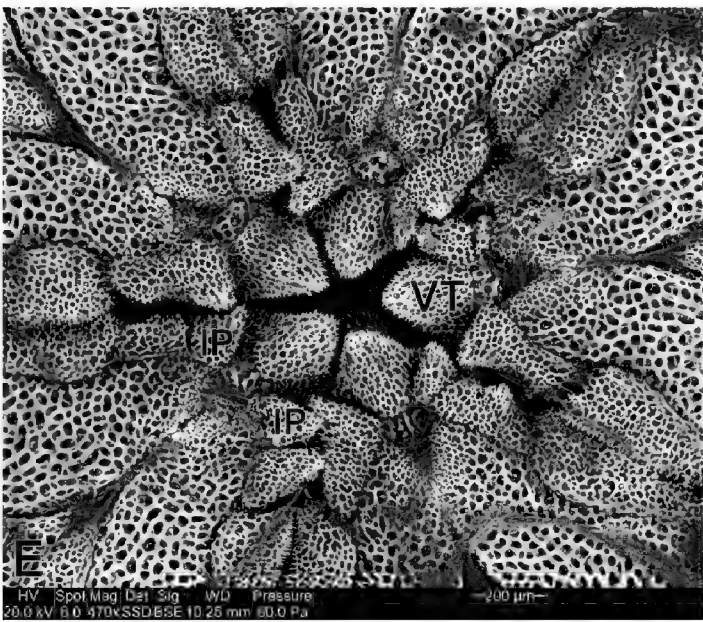
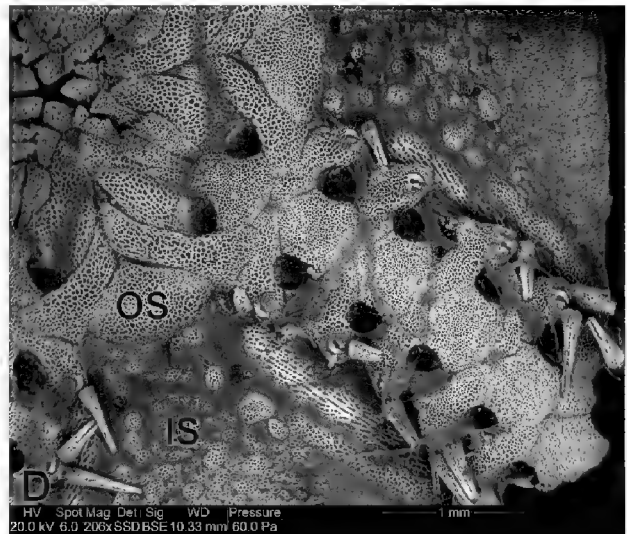
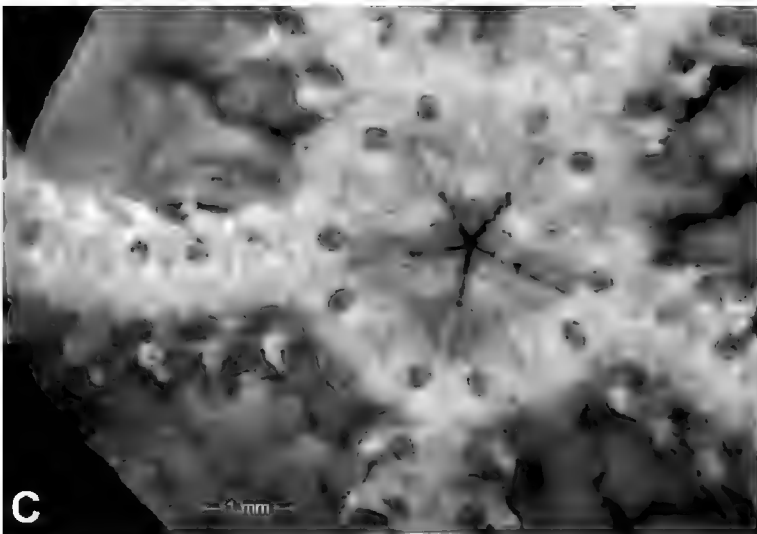
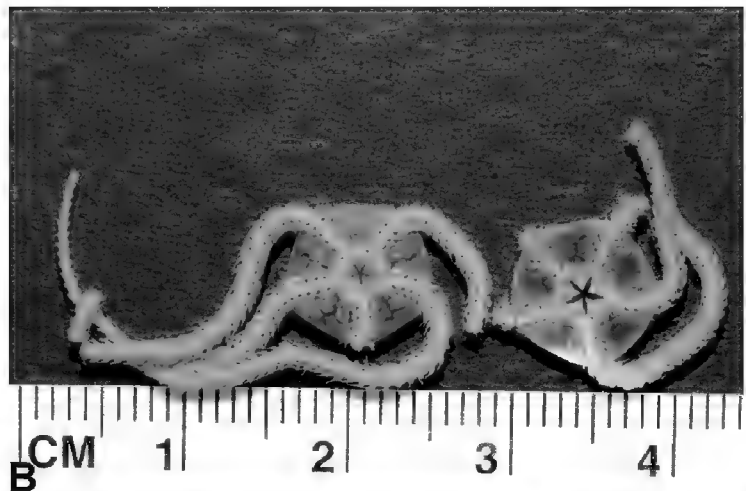


Figure 14. *Amphilepis platytata* **A** museum label **B** ventral view of two preserved specimens, arms with many short segments, 4-5 arm segments within disk **C** mouth area before SEM preparation **D** SEM of mouth area and proximal arm segments, triangular oral shields, sparse interbrachial scales, no tentacle pore scales **E** SEM of mouth area with pointed ventral teeth and infradental papillae **F** SEM of 7 arm segments partially bleached, VAPs nearly pentagonal, no tentacle pore scales, ventral, distal left. Abbreviations as in Fig. 12.

scale on lateral side of underarm-plate"); *A. platytata* has no tentacle scales (Figs 14C, 15A, B), which agrees with Clark's 1911 original description of a single 8.0 mm dd specimen, (2) *A. patens* has disk covered above and below with translucent scales, as described by Lyman (1879) (Fig. 12C, D, F); in *A. platytata* the ventral interbrachial

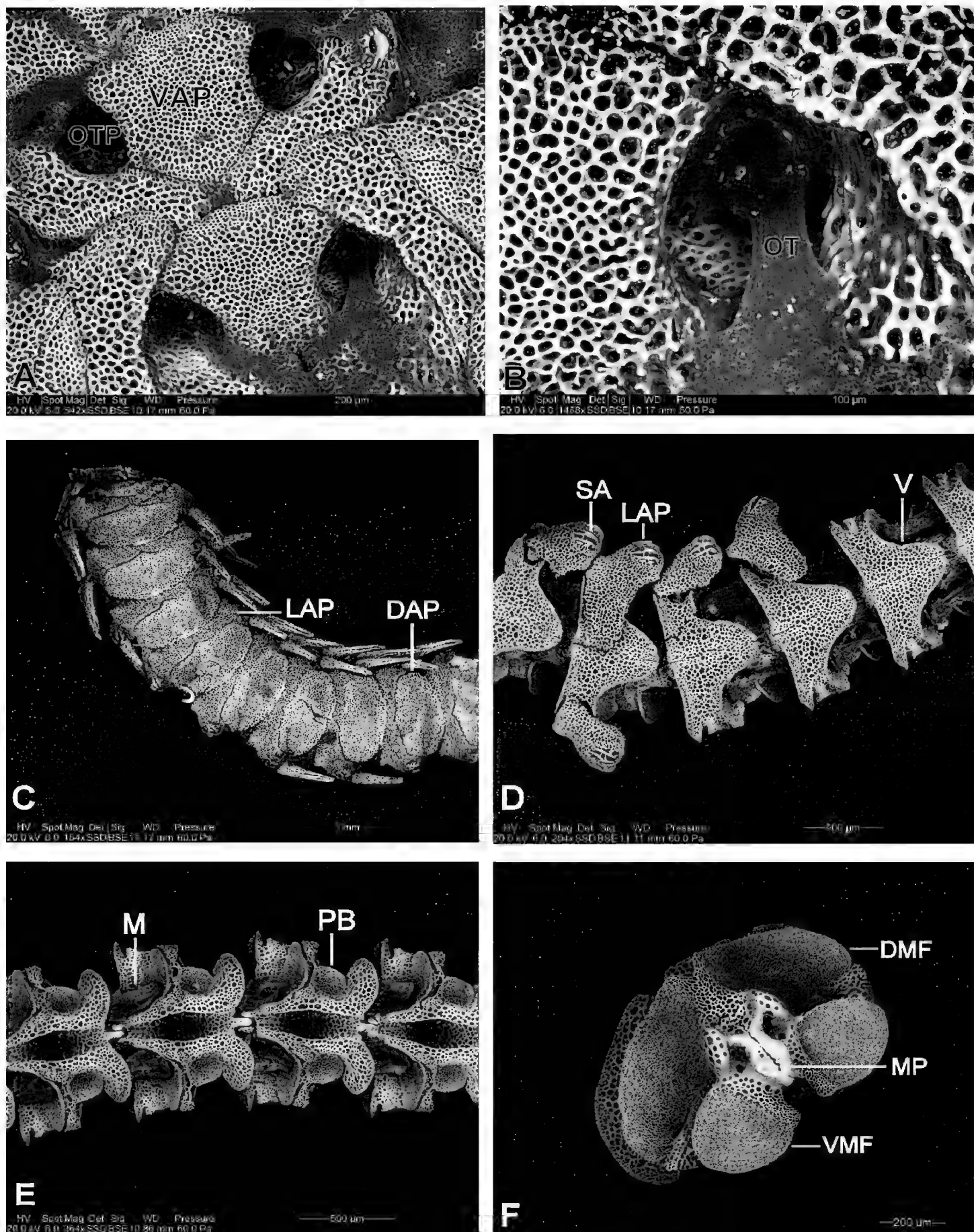


Figure 15. SEMs of *Amphilepis platytata* **A** enlarged view of mouth area in Fig. 14D, oral tentacle pores without scales **B** oracle tentacle inside tentacle pore, no scales **C** partially bleached string of 8 arm segments, broad DAPs and LAPs, dorsal, distal right **D** bleached string of vertebrae, spine articulations on LAPs, dorsal, distal right **E** string of 4 vertebrae with muscles connecting flanges, ventral, distal right **F** distal face of proximal vertebra showing muscle flanges, median process, and articulating surfaces. Abbreviations as in Fig. 12 plus: DMF – dorsal muscle flange, M – muscle, MP – median process, OT – oral tentacle, OTP – oral tentacle pore, PB – podian basin, VMF – ventral muscle flange.

spaces are sparsely covered with small scales (Fig. 14D), as described by Clark (1911), and (3) *A. patens* has ventral teeth broadly rounded (Fig. 12C–E) and infradental papillae elongated along the adoral shields (Lyman 1879: “mouth papillae broad and irregular; on either side of the large prominent mouth-angle, at the outer corner, are two more or less closely joined; and, at the apex, a larger pair which, through the gap between them, show the small lowest tooth”); *A. platytata* has ventral teeth and infradental papillae pointed toward mouth opening (Fig. 14C–E), as described by Clark (1911), “Oral plates large, each carrying two low wide, truncate papillae. Teeth nearly triangular.” While Pomory et al. (2011) suggested that “Amphilepidids have triangular teeth,” this is not the case for *A. patens*. The shape of ventral teeth was not mentioned by O’Hara et al. (2018) as a trait for Amphilepidida, Amphilepididae, or Amphiuridae.

Morphology of *Ophiophragmus filograneus*

The *Amphilepis* species above were examined because of their close taxonomic relationship to *Amphicutis*. The species *Ophiophragmus filograneus* (Figs 16A–F, 17A–F) was examined primarily because it lives in organically rich sediments in estuaries of Florida (USA) with brackish water (Turner and Meyer 1980); salinity ranges there are near or below those of Bernier Cave. Since the low salinity of Bernier Cave probably contributes to the reduced stereom of *A. stygobita*, it is surprising that the stereoms of my *O. filograneus* SEMs (Figs 16A–F, 17A–F) are not reduced as much as those of *A. stygobita*.

Discussion

Feeding on detritus with EPS, skin may absorb DOM or EPS

While the types of food consumed by brittle stars may be determined by examining food in stomachs of preserved and dissected specimens, the actual feeding process of many brittle stars is unknown, especially for species like *A. stygobita* that consume detritus and for species in certain families. For instance, according to Hendler (2018), “the feeding behavior of Amphilepididae is an enigma.” So, the feeding behaviors of *A. stygobita* (family Amphilepididae) provide valuable insight for this group. This species ignored or rejected foods that are often fed to other brittle stars, including boiled egg, boiled lettuce, shrimp, fish, and TetraMin© fish flakes. Instead, they fed exclusively on cave detritus which they consumed while nearly flat on the surface of the detritus, occasionally with disk partly buried, but not with arms raised above the detritus the way passive suspension feeders collect particulate matter from the water (Hendler 2018).

Captive *A. stygobita* pulled fresh detritus into the mouth with their oral tentacles (Fig. 3C, D, 90 sec. apart) and without masticating or closing the mouth. In fact, live *A. stygobita* always had their mouths open whenever I observed or photographed their oral surfaces (Figs 3C, D, 4A–F, 6E). There appeared to be no selection or filtering of the various detritus components as they streamed into the mouth. This stream of detritus

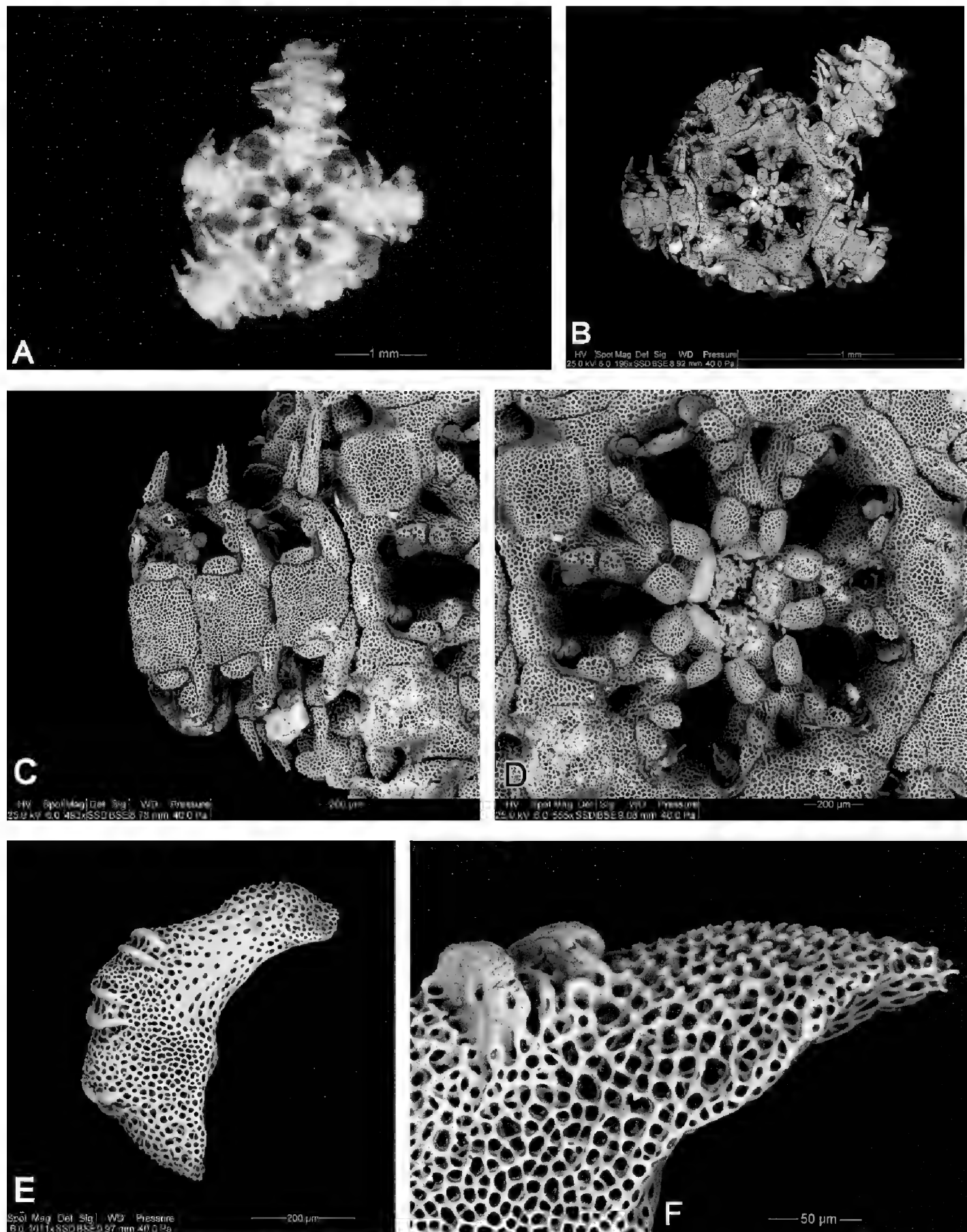


Figure 16. *Ophiophragmus filigraneus* **A** ventral view of disk and mouth area before bleaching, buccal funnel **B** lightly bleached SEM of disk and mouth area **C** SEM of 3 arm segments, wide VAPs and LAPs **D** SEM of mouth area **E** LAP with 3 spine articulation sockets with parallel sides **F** LAP with thick raised lobes of spine articulation.

was part of a sticky biofilm mass. It is not uncommon for caves to have phototrophic biofilms that are held together by extracellular polymeric substances (EPS), and for these EPS to be produced mainly by cyanobacteria and diatoms (Roldán and Hernández-Maríné 2009; Falasco et al. 2014). Not only did this biofilm help hold detritus

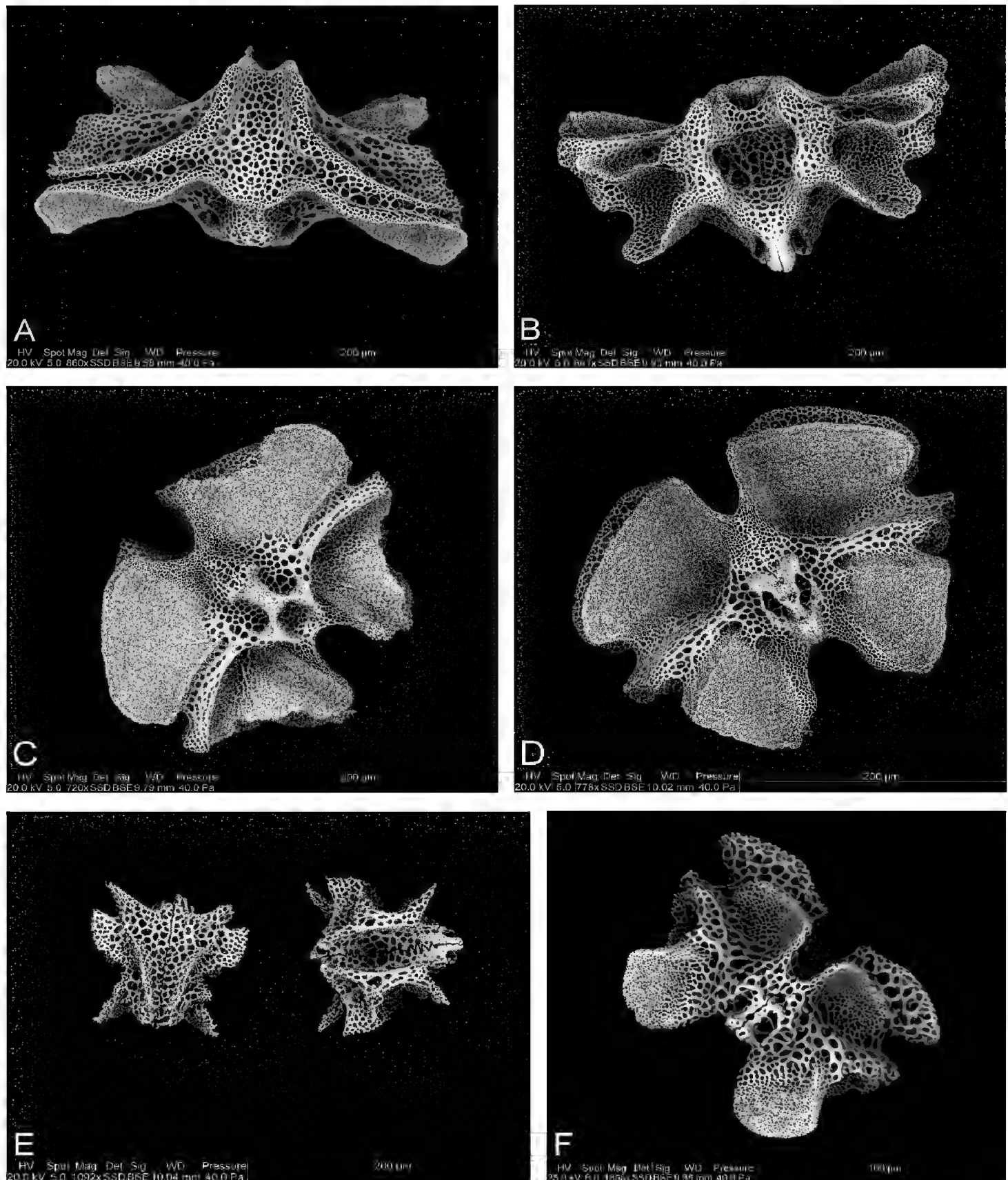


Figure 17. SEMs of *Ophiophragmus filigraneus* **A** dorsal view of vertebra near disk, width $2 \times$ length and moderately fenestrated **B** ventral view of vertebra near disk, wide and fenestrated, elongated median process **C** proximal face of vertebra from near disk, arches radiate outward from ventral processes **D** distal face of vertebra from near disk, arches radiate outward from dorsal processes **E** dorsal (left) and ventral (right) views of vertebrae from near distal end of arm, width nearly same as length **F** distal face of vertebra from near distal end of arm, more fenestrated than proximal vertebrae.

together for easier manipulation by *A. stygobita*, it probably provided significant additional nutrients since such biofilms are composed of polysaccharides, proteins, lipids and nucleic acids (Falasco et al. 2014). Hoskins et al. (2003) studied the utilization of algal and bacterial EPS by the deposit-feeding brittle star *Amphipholis gracillima*

(Stimpson, 1854) and suggested that “EPS may represent a significant energy source for this deposit-feeding ophiuroid and other organisms with similar feeding habits. Additionally, *A. gracillima* appears to be especially adept at utilizing EPS resources from benthic diatom communities.” Sköld and Gunnarsson (1996) also found that the two detritus-consuming brittle star species, *Amphiura filiformis* (OF Müller, 1776) and *Amphiura chiajei* Forbes, 1843, were capable of increasing their growth and gonad development in response to short-term organic enrichment with concentrated diatoms. Large marine diatoms such as *Campylodiscus* are particularly good producers of EPS (Shnyukova and Zolotariova 2017). The substantial population of *C. neofastuosus* was probably a large contributor to the EPS in Bernier Cave detritus. Bruckner et al. (2011) found that the release of EPS by benthic diatoms depends on interactions with bacteria.

Hendler (2018) indicated that, “Two principal feeding modes of ophiuroids, macrophagy and microphagy, are distinguished according to the type of food consumed and manner in which it is acquired (reviewed by Warner, 1982). Generally, macrophagous species are carnivores and carrion feeders that grasp prey in loops of their arms, whereas microphagous species are deposit feeders and passive suspension feeders that gather particulate material with their tube feet.” It is clear that *A. stygobita* is a microphagous deposit feeder. The discussion of “feeding adaptations of microphagous ophiuroids” in Hendler (2018) concentrated on passive suspension feeders such as *Ophiothrix spiculata* LeConte, 1851, whose anatomy and feeding behavior are much different from that of the detritus feeding *A. stygobita*. Feeding behaviors of *Ophiothrix* species include: directing the ambulacral surfaces of raised arms toward the current, using tube feet to accumulate particulate material that they bind into a bolus, and moving the bolus toward the mouth where oral tentacles push the bolus through the buccal funnel as jaws open and close (Hendler 2018). The specialized tube feet and buccal funnel distinguish *Ophiothrix* species from macrophagous species; several other species have similar feeding behaviors and buccal funnels (Hendler 2018). Thus, it is important to visualize the buccal funnel described by Hendler (2018) as a funnel-shaped complex feeding apparatus that comprises a graduated series of oral papillae on the jaws and surrounded by radiating spindle-shaped oral slits between the jaws. Included in this paper are digital light microscope photos and SEMs of buccal funnels of three species to compare to *A. stygobita*, which does not have a buccal funnel: *Ophiophragmus filigraneus* (Fig. 16A, B, D), *Ophiophragmus wurdemanii* (Lyman, 1860) (Fig. 18A), and *Ophiomastix wendtii* (Müller & Troschel, 1842) (Fig. 18B).

Compared to most other species such as *Ophiophragmus filigraneus* (Fig. 16B), *Ophiophragmus wurdemanii* (Fig. 18A), and *Ophiomastix wendtii* (Fig. 18B), the oral frame ossicles of *A. stygobita* are reduced in number, highly variable, highly fenestrated, and loosely organized. In fact, the teeth and most oral papillae that would normally be used by most species for masticating or swallowing food appear to be missing or so fenestrated that this species may have difficulty manipulating food other than soft detritus. This appears to be another energy-saving feature used by *A. stygobita* because more complex mouthparts are not needed for microphagous detritus feeding. O’Hara et al. (2018) considered reduced or absent tooth clusters and reduced skeletons to be pedomorphic traits.

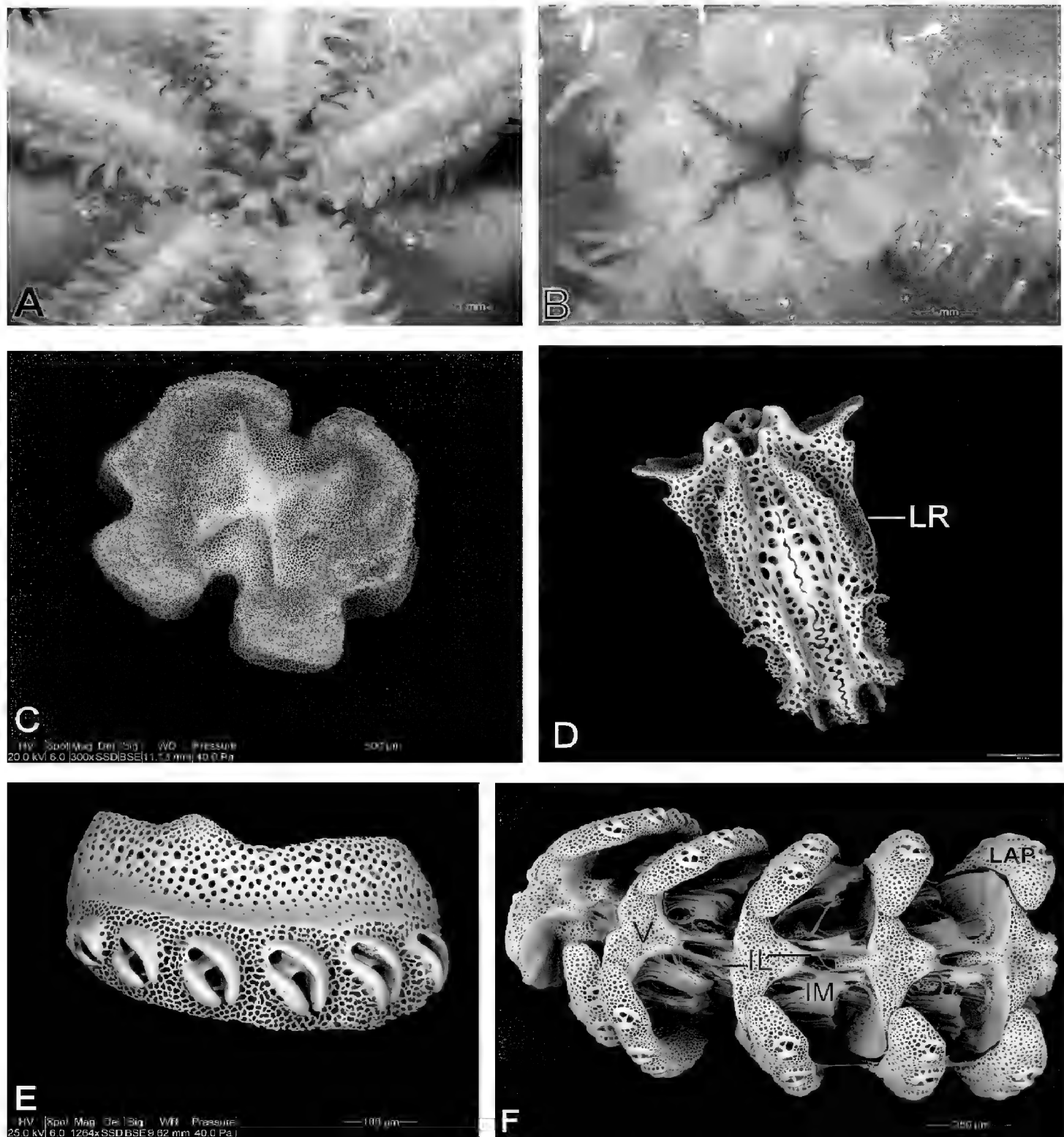


Figure 18. Miscellaneous morphological features for comparisons **A** preserved *Ophiophragnus wurdemanii*, mouth with buccal funnel **B** live *Ophiomastix wendtii*, mouth with buccal funnel **C** SEM of *Asteroschema brachiatum* proximal vertebra end, hourglass-shaped streptospondylous articulation **D** SEM of mid-arm vertebra of *Ophiocomella sexradiata*, ventral, with lateral ridges for connections to VAP **E** SEM of LAP of *Ophiothrix angulata*, 6 thick spine articulation lobes oriented diagonally **F** SEM of *Ophiactis savignyi* string of 5 pairs of very wide LAPs attached to Vs with intervertebral muscles, Vs attached to Vs with ligaments. Abbreviations: IL – intervertebral ligaments, IM – intervertebral muscles, LAP – lateral arm plate, LR – lateral ridge, V – vertebra.

The generic epithet *Amphicutis* (= around skin) was given to this cave brittle star because it has a translucent layer of skin raised above the surface of arms that persists after calcification (Pomory et al. 2011) (Fig. 3F). Pomory et al. (2011) speculated that this species may feed on dissolved organic matter (DOM), and the soft tissue might improve absorption of DOM, since other brittle stars are

known to use DOM (Clements et al. 1988). The fact that *A. stygobita* is a detritus feeder does not exclude the possibility that absorption of DOM and EPS by the skin might provide additional nutrients.

Reproduction and development of babies

Pomory et al. (2011) indicated that *A. stygobita* appeared to have spawned (to produce developing larvae externally) soon after being collected, but that observation was obviously incorrect, since three babies born in 2018 showed that this is a brooder instead of a spawner. Hendler (1975) indicated that only about 55 species, or about 3% of approximately 2000 species of ophiuroids, had been reported as brooding, although the reproductive mode of many other species is unknown and additional species may be recognized as brooding (Hendler et al. 1995; Stöhr 2005). Table II in Hendler (1991) indicates about 69 species are brooders. The birth of three *A. stygobita* babies confirms that this species is another brooder.

Gonads and developing embryos were visible in most adult *A. stygobita*. Horizontal serial sections revealed that both testes and ovaries were present in the same specimen indicating hermaphroditism. Hendler (1975) suggested that the high occurrence of hermaphroditism in viviparous ophiuroids may be “a function of the relatively inefficient dispersal of these forms,” and hermaphroditism ensures both sexes to be present “in newly settled areas with low population density.” This corresponds to the difficulty for a cave endemic brittle star to disperse and to the apparently low population of *A. stygobita* in the two caves it is known to inhabit. However, the populations of *A. stygobita* could be much larger than they seem since individuals are difficult to find with their very small disks that are usually filled with detritus so they are camouflaged by the surrounding detritus. Babies would be even more difficult to find in the detritus because they are microscopic (dd = 0.8 mm), as well as camouflaged. Since adults have relatively few ovaries and embryos, reproduction would seem to be slow, which is typical of cave adapted animals (Culver and Pipan 2019).

Brooding in *A. stygobita* appears to take place within the ovaries since bursae could not be identified in this study, nor in dissections done for the original description (Pomory et al. 2011). Hendler (1975) discussed various locations for brooding, including: within bursae, within ovaries, beneath the disk in *Ophiophycis gracilis* (Mortensen, 1933), and on the oral surface of the arms in *Astrotoma waitei*, now *Astrothorax waitei* (Bonham, 1909). Hendler (1975) noted that *Ophiophycis* (dd ~2 mm) “is among the smallest of ophiuroids and its 10 eggs, each 0.15 to 0.20 mm in diameter could conceivably be too large for bursal brooding, hence external brooding.” This same phenomenon may help explain the intraovarian brooding of *A. stygobita*, which is very small (dd = 3–4 mm) with relatively large eggs and developing embryos 0.20 to 0.35 mm. Although pre-released embryos may be only 0.35 mm, it is likely that newly released babies with 0.8 mm dd and arms of 0.6 mm could result from a 0.35 mm embryo unfolding. The length of time for egg and embryo development in *A. stygobita* appears to be greater than 1 year, since several adults showed little change in ovaries during this amount of time in captivity.

This corresponds to the slow growth rates observed in adult regeneration experiments (Carpenter 2016) and slow growth of babies in the current study.

As noted in Results section, if central and radial primary plates were present in disks of the three babies, they were obscured by disk scales (Fig. 5E). Stöhr and Martynov (2016) said “primary plates seem to have been lost completely (not just in adults), several times independently on species level in several families.”

Babies were born with LAPs well developed to support the 2 arm segments, while dorsal arm plates appeared to be absent (Fig. 5B–D); ventral arm plates were not easily viewed on the ventral side of the tiny babies. Based on their study of ophiuroid ontogeny, Stöhr and Martynov (2016) indicated that, “Dorsal arm plates are at first absent and develop gradually, starting on the proximalmost joints. Of the ventral arm plates the first one is always present from the youngest stages as part of the mouth frame, while the following develop gradually, but usually before the corresponding dorsal plate.” Stöhr and Martynov (2016) also said that, at the 2-3 arm joint stage, the arms are formed by joined pairs of lateral plates and bear two spines. It appears that *A. stygobita* follows this same pattern of arm development, starting with LAPs and Vs, followed by proximal VAPs, then DAPs.

As noted in Results section, babies were born with disk diameters of ~0.8 mm (adults have ~4 mm dd) and the number of segments per arm was very small for a brooding species, with only 2 arm segments. According to Hendler (1975), newly hatched young of viviparous species range from 0.6 to 5.0 mm dd and have 8 to 40 arm segments, and “the major limitation on size for brooded young appears to be the size of the parent.” Stöhr (2005) provided descriptions and SEM images of small juveniles of 17 ophiuroids, including three brooding species: *Ophiomitrella clavigera* (Ljungman, 1885) (smallest free-living juveniles had 1.5 mm dd and 13 arm segments), *Ophiacantha anomala* GO Sars, 1871 (smallest free-living juveniles had 2.0 mm dd and > 8 arm segments, and *Amphiura borealis* (GO Sars, 1871) (smallest free-living specimen had 0.7 mm dd and 5-6 arm segments). Byrne (1991) reported that adult *Ophionereis olivacea* HL Clark, 1900 with a maximum dd of 5.2 mm had juveniles emerge from the bursae at 0.48 mm dd and each arm had three segments. Even though *A. stygobita* babies were born with larger disks than *O. olivacea* (0.8 vs. 0.48 mm), the relatively fewer segments (2 vs. 3) is consistent with adult *A. stygobita* having fewer segments than adult *O. olivacea*.

Since *A. stygobita* babies and adults have relatively few segments, they have fewer joints in each arm, which makes it more difficult for them to use the normal brittle star mode of walking by bending the arms. As a result, adults and babies of this species were observed to move primarily by podial walking, which is common in asteroids (e.g., sea stars) but not in brittle stars (Carpenter 2011; Pomory et al. 2011; current study). Stöhr et al. (2012) said, “Ophiuroid tube feet lack suction cups and are rarely used for locomotion. Instead, ophiuroids move by twisting and coiling their arms, pushing against the surface like a snake or gripping objects and pulling themselves forward.” However, podial walking is typical of baby brittle stars because they have relatively short arms with few segments and joints, and since adult *A. stygobita* have short arms with few segments and joints, they would tend to use podial walking as well.

According to Stöhr and Martynov (2016), “arm segments are relatively longer in juveniles than in adults, but adult distal arms are similar to juvenile arms, because the arms grow at the tip, proximal to the terminal plate, and thus the distal part is younger and less developed than the proximal part. Growth occurs first lengthwise, later widthwise.” The first two arm segments of *A. stygobita* babies are also relatively longer than segments in adults; baby arm segment length/dd ($= 0.2 \text{ mm}/0.8 \text{ mm}$) $= 25\%$, while adult arm segment length/dd ($= 0.6 \text{ mm}/4.0 \text{ mm}$) $= 15\%$. These segment lengths of $\sim 0.2 \text{ mm}$ in babies (Figs 5B–D, 6A–E) and $\sim 0.6 \text{ mm}$ in adults (Figs 3A, 5A) are rather uniform except at distal ends where segments may be shorter while being produced (Figs 3B, 6E). This means that dd increases 5-fold (4.0 mm in adults/ 0.8 mm in babies), while segment length increases only 3-fold (0.6 mm in adults/ 0.2 mm in babies) during a lifetime. The width of arm segments in adults varies considerably near distal ends, being relatively narrow when segments are first produced (Fig. 10B) and increasing more in width than in length during their lives. On the other hand, the first 2 segments of *A. stygobita* babies were relatively wide, with the greatest width near distal ends of segments being nearly as wide as long. In this respect, the very narrow adult distal arm segments are very much different from the very wide first arm segments of babies.

Developing Vs were visible inside the two segments of babies; the most apparent vertebral structures were the 2 parallel ambulacral plates that eventually form support for adjoining parts (Figs 5B–D, 6B–F). *Amphicutis stygobita* babies were kept alive as long as possible to provide valuable information on development and behavior; unfortunately, they were not available for SEM study of their ossicles since they disintegrated soon after dying.

Growth rates

As noted in the results section, two adult *A. stygobita* were observed to regenerate arm tips at a rate of up to 1 mm in 24 weeks (Carpenter 2016). This is one of the slowest regeneration rates reported for any brittle star species with several possible contributing factors mentioned by Carpenter (2016). In the current study, babies also had a very slow growth rate; arm length increase of baby #2 was only $\sim 0.2 \text{ mm}$ (from ~ 0.6 to $\sim 0.8 \text{ mm}$) in 13.5 months (Fig. 6E). At this growth rate of $\sim 0.1 \text{ mm/yr.}$ for dd and $\sim 0.2 \text{ mm/yr.}$ for arms, it would take about 30–40 years to reach the size of adults we have collected. Of course, growth rates in nature could be considerably faster with a better, fresher supply of detritus for food. In comparison, two adult specimens were observed to regenerate arm tips at a rate of up to 1 mm in 24 weeks (Carpenter 2016), which is about 12 times faster than growth in baby #2 ($0.2 \text{ mm}/13.5 \text{ mo.} = 0.08 \text{ mm}/24 \text{ wks.}$). However, baby growth and adult regeneration rates were somewhat closer if relative sizes are compared: dd of babies were 0.8 mm and adults were 4 mm ($= 5$ times as large), and growth rates may not be comparable to regeneration rates in the same species.

In contrast to the slow growth of *A. stygobita* babies, Gage (1984) observed that postlarvae and juveniles of non-brooders initially grow quickly. Ravelo et al. (2017) indicated that the growth curves of two continental shelf brittle stars from Alaska, *Ophiura sarsii* Lutken, 1855 and *Ophiocten sericeum* (Forbes, 1852), had “initial fast

growth, with an inflection period followed by a second phase of fast growth” and with maximum ages of 27 for *O. sarsii* and 20 years for *O. sericeum*. These growth patterns and ages were determined using annual growth bands on muscle flanges (fossae) of Vs as described by Gage (1990). Similar growth bands can be seen in the muscle flanges of *Amphilepis patens* (Fig. 11E, F), *Amphilepis platytata* (Fig. 15F), and *Ophiophragmus filograneus* (Fig. 17C, D). One reason I started using SEM was to look for growth rings in *A. stygobita*, but their highly fenestrated Vs did not display any distinguishable growth rings (Fig. 11A–D), and Gage (2003) indicated that it was difficult to find growth rings on specimens with dd less than ~5 mm because “the small overall size of the ossicle in relation to its mesh-like microstructure did not allow differences in surface relief or stereom density to be as easily recognizable as in other species.”

Morphology of adult *A. stygobita* compared to other species

Several morphological features of *A. stygobita* are quite extraordinary. To compare SEMs of *A. stygobita* to those of other species, SEMs of many epigean brittle star species have been published; some of the most extensive include: Sumida and Tyler 1998; Stöhr 2005; Stöhr et al. 2012; Stöhr and Martynov 2016; Hendler 2018; O’Hara et al. 2018. Included here are my own SEMs of a few species selected from more than 20 that I prepared for comparison to *A. stygobita*.

Taxonomic considerations: *Amphilepis patens* and *Amphilepis platytata*

When *A. stygobita* was described by Pomory et al. (2011), its traits were distinctive enough to create the new genus *Amphicutis*. However, it was difficult to decide what family to place it in because it has some traits of Amphiuridae, some traits of Amphilepididae, some in between, and some unique. The decision was made to place this species in the family Amphilepididae, but that decision was considered tentative. Family placement remained uncertain (“incertae sedis”) in the taxonomic revision by O’Hara et al. (2018) since they did not have tissue from *A. stygobita* for molecular analysis; however, they did move the families Amphilepididae and Amphiuridae from the order Ophiurida to the order Amphilepida. O’Hara et al. (2018) commented that the large family Amphiuridae requires revision and, “Preliminary findings (O’Hara et al. 2017) indicate that there are at least three major clades within the group that fit our criteria for family status.” They also remarked that the family Amphilepididae “is a paedomorphic family with reduced characters.” The following discussion may help resolve these family issues in the future.

The oral frame features in SEM images of *A. stygobita* (Figs 8A–C, 9) show some key traits, most of which were described by Pomory et al. (2011) as follows. (1) The ventral tooth at the apex of each jaw is broadly rounded, rather than triangular as in most other amphilepidids (triangular in *A. platytata*, rounded in *A. patens*), (2) oral plates are blunt ended as in amphiurids, rather than pointed as in amphilepidids (including *A. patens* and *A. platytata*), (3) the 2nd tentacle pore (= 1st tentacle pore visible in ventral view) of the oral frame is outside mouth slit as in most amphilepidids, including *A. platytata* (Fig. 14D),

but inside (or even with distal ends of slit) in *A. patens* (Fig. 12C–E), while most amphiuroids have it inside the mouth slit, (4) oral shields are small and oval, similar to disk scales in appearance (usually triangular, sometimes diamond or heart shaped in *Amphilepis*), (5) lateral arm plates (LAPs) within the disk have large indentations on the ventral surface to partially encompass lateral edges of podial pores, and ventral arm plates are figure-8 shaped to partially encompass medial edges of podial pores (Fig. 8A–C), which seems to be unusual since it does not appear in any figures in Pomory's (2007) key, and (6) disk contains either 2 arm segments with LAPs distal to plates bounding end of mouth slit at (CP1 and CP3 in Fig. 8A), or 1.5 arm segments (CP 11 in Fig. 8A) or only 1 arm segment (CP6, Fig. 8A; CP8, Fig. 8A, C). This last trait differs from the original description (Pomory et al. 2011), "Three arm segments with lateral plates distal to plate bounding end of mouth slit on ventral side of disk." Whether the number of arm segments within the disk is 2, 1.5, or 1, the number is unusually small. For comparison, Pomory's (2007) taxonomic key illustrated 13 common genera, all with 3 to 7 arm segments within the disk; only *Ophiostigma* had 3, 2 genera had 4, 8 genera had 5, and 2 had 7. The number of arm segments within the disk may have relatively little taxonomic value, since Pomory (2007) did not mention or use it in his key, nor is it consistently mentioned in descriptions of new species. However, the low number of 1–2 segments within the disk corresponds well with the relatively low number of ~10–20 arm segments outside the disk.

One reason the two deep-sea *Amphilepis* species were examined was to compare their possible paedomorphisms to those of *A. stygobita*. The mouth features in all three species appear to be somewhat reduced (paedomorphic), especially in the number of oral papillae; however, the papillae seem to be more variable and less defined in *A. stygobita* (Figs 9, 12E, 14E), perhaps due to variable calcification states. The reduction in trabeculae and corresponding increase in fenestration are greater in *A. stygobita* and are especially noticeable in LAPs and Vs (Figs 8A, 11C, vs. 11E, 13D, 15D–F).

Salinity considerations: *Ophiophragmus filograneus*

Considering that *A. stygobita* and *O. filograneus* both live in low salinity environments, it is surprising that the stereoms of my *O. filograneus* SEMs (Figs 16A–F, 17A–F) are not reduced as much as those of *A. stygobita*. This may be partly because my *O. filograneus* specimen was considerably larger (dd = 8 mm) than my *A. stygobita* specimens (dd = 3–4 mm). A study by LaFace (2019) confirmed that reduced salinity can result in reduced ossicles with greater fenestration. LaFace (2019) found that regenerating arm ossicles of *Amphipholis squamata* maintained at ~25 ppt had "thinner ridges and less pronounced trabeculae than the regenerated ossicles of the brittlestars in the control condition." LaFace (2019) noted that "the stroma was also more elongated at day 28 so the shape resembled ovals rather than circles." Donachy and Watanabe (1986) found that length of regenerated arms and number of ossicles formed in *Ophiothrix angulata* were significantly less at 23 ppt than at 28–38 ppt; they correlated this with reduced calcium concentrations at lower salinities. Other traits of *O. filograneus* are compared to *A. stygobita*'s in the following pages comparing anatomies.

Anatomy of arm segments

In their original description, Pomory et al. (2011) noted the unusual arm segment anatomy, “The dorsal and ventral arm plates of most ophiuroids are typically large and in contact, or nearly in contact, in sequence along the length of the arm. The lateral arm plates are usually small and separated from one another across an arm. The new species has the exact opposite arrangement. The dorsal and ventral arm plates are small and distinctly separated from one another along the length of the arm with the lateral arm plates large and broadly in contact across an arm. No shallow-water Caribbean species has this character as an adult.” SEM images of *A. stygobita* (Figs 7–10) confirm this unusual arrangement of segment ossicles, which effectively reduces weight but retains strength. Especially note that elongated LAPs almost completely encompass Vs and provide strength for arm segments, in conjunction with lateral extensions to Vs. This results in LAPs that are oriented parallel to the vertebral axis, comparable to splints used to stabilize a human broken arm. In contrast, many species have heavy LAPs extending laterally and supporting several spines pointing distally or laterally to provide protection from predators and to grip the substrate to help them move forward as they swing arms. Examples include: *Amphilepis patens* (Fig. 13A, C, E), *Amphilepis platytata* (Figs 14C, E, 15C, D), *Ophiophragmus filograneus* (Fig. 16A–C), and *Ophiactis savignyi* (Müller & Troschel, 1842) (Fig. 18F).

Amphicutis stygobita is unusual in having only two spines which are near the end of LAPs (Fig. 7D, E). Pomory et al. (2011) indicated that, “Only one other shallow-water Caribbean species in a different family, *Ophiolepis paucispina* (Say), consistently has only two arm spines (Hendler et al. 1995; Pomory 2007).” Arm spine articulations in *A. stygobita* are nearly round with 2–3 openings for muscles and nerves to pass through to the spine; lobes are only slightly raised (Fig. 7F). This type of spine articulation appears to be unusual, since O’Hara et al. (2018) included in their diagnosis of the order Amphilepidida (which they created in O’Hara et al. 2017), “Dorsal and ventral lobes of arm spine articulations parallel (except in Ophiotrichidae).” This parallel arrangement is seen in my other specimens in the order Amphilepidida: *Amphilepis patens* (Fig. 13D–F), *Amphilepis platytata* (Fig. 15D), *Ophiophragmus filograneus* (Fig. 16E, F), and *Ophiactis savignyi* (Fig. 18F). In contrast, *Ophiothrix angulata* (Say, 1825) (family Ophiotrichidae, order Amphilepidida) has thick spine articulation lobes oriented diagonally (Fig. 18E). The reduced number of spines and shallow arrangement of spine articulations in *A. stygobita* may be the result of the overall reduction in stereom density, which provides additional energy conservation.

Anatomy of vertebrae

Stöhr and Martynov (2016) concluded, “It is clear that species in which adults have vertebrae with a L:W ratio below 1 are well developed, whereas species with values close to 10 are strongly paedomorphic.” Of course, it depends on the technique used to measure Vs and on which Vs are measured since distal ones tend to be much narrower

than ones near the disk. Nevertheless, the L:W ratio of *A. stygobita* Vs (Figs 8F, 10A, B) is in the upper part of this paedomorphic range, and it is much greater than most species, including most deep sea paedomorphic species such as *Amphilepis* species.

Lateral extensions of Vs in *A. stygobita* connect with LAPs; some Vs have 3–4 narrow extensions on each side (Fig. 7C), some are flared or knobbed to form wider attachment points to LAPs (Figs 8D, 10A), and some form interrupted ridges for attachment points (Figs 8F, 10E). Other species with elongated Vs often have lateral ridges that connect to LAPs as in *Ophiocomella sexradiata* (Duncan, 1887) (Fig. 18D). Several families of ophiuroids (e.g., Ophiopsilidae, Amphilimnidae, and Amphiuridae) have the inner side of LAPs with two, three, or more merged knobs instead of a ridge to connect to Vs (O'Hara et al. 2018). The very narrow Vs at the distal ends of arms of *A. stygobita* have short lateral extensions (Fig. 10B), indicating they lengthen as Vs widen.

Since Vs and LAPs of *A. stygobita* are very narrow, there is less surface area on ends of Vs and LAPs to form connections to adjoining Vs and LAPs. For comparison to the very narrow segments of *A. stygobita*, please note the very wide segments of *Ophiactis savignyi* (Duncan, 1887) (Fig. 18F); muscles and ligaments between segments were left intact to show how adjoining LAPs connect with each other along their length, and Vs have large areas of connections to adjoining Vs.

Irimura and Fujita (2003) observed that, “Two morphological types of the vertebral articulation, streptospondylous and zygospondylous, have been traditionally used by many taxonomists to classify ophiuroids into separate orders or suborders.” However, O'Hara et al. (2018) noted that, “Arm vertebrae are subject to ecological adaptation and show convergent evolution. This character cannot therefore be used on its own but it is helpful in combination with other characters or to differentiate closely related groups.” Streptospondylous articulations are hourglass-shaped (Fig. 18C), both proximally and distally, that give great arm joint flexibility that allow arm loops and coils characteristic of gorgonocephalids (e.g., basket stars) (LeClair 1996). The zygospondylous type of articulation is more mechanically limited and has vertebral surfaces bearing a complex set of projections and depressions that fit into the complimentary articulating surfaces of the adjacent V; this is typical of most brittle stars (LeClair 1996). Articulations in *A. stygobita* are zygospondylous but are significantly modified compared to most species.

The connections of Vs in *A. stygobita* are different from other species in several ways. The median socket is thinner and the median process is thinner and more pointed (Fig. 11 C, D) in comparison to *Amphilepis patens* (Fig. 11E, F) and *O. filograneus* (Fig. 17C, D). The muscle flanges, dorsal processes, and ventral processes at the ends of *A. stygobita* segments are not only relatively small, they are also highly fenestrated; please compare these structures in *A. stygobita* (Fig. 11C, D), *Amphilepis patens* (Fig. 11E, F), and *O. filograneus* (Fig. 17C, D). In *O. filograneus* the Vs that are early in development near distal ends of arms (Fig. 17F) are similar to more proximal Vs in *A. stygobita* (Fig. 11C, D). Although strong fenestration might provide better attachment for individual muscle fibers, it probably creates joints that are weaker and less flexible, which could result in reduced capability to move arms forward and contribute to the tendency to use podial walking. Individual tube feet of *A. stygobita* are very large with an enlarged

smooth knob on the end and 2-3 rings/ridges below knobbed end (Pomory et al. 2011). The large podian basins on the ventral surfaces of Vs (Fig. 8 E, F) provide space for the large podia. The weakness in arm joint articulation structure may be partly compensated for by multiple connections between Vs and LAPs to hold segment ossicles together.

Highly fenestrated ossicles

The ossicles of *A. stygobita* (including disk scales, Vs, LAPs, and other arm components) are highly fenestrated with a net-like lattice around larger open spaces, more than in *O. filigraneus* (Figs 16C–F, 17A–F) and other species I have examined. One of the distinctive traits of the genus *Amphicutis* described by Pomory et al. (2011) is that the “disk and arms are often formed by soft tissue outlining plates and scales but lacking significant calcification,” and “the soft tissue creates up to 13 arm segments with just a thin axial center of calcium carbonate.” Apparently, the highly fenestrated ossicles seen in SEM’s correspond to this lack of calcification, which seems to be at a greater extent than in other brittle star species. Pomory et al. (2011) suggested that the soft tissue-calcification differences may be a paedomorphic trait.

Paedomorphism advantages

Paedomorphic traits have been mentioned several times in this paper. Probable reasons for why ophiuroid paedomorphic traits occur are usually not explained in other papers. For instance, O’Hara et al. (2017) described various taxonomic groups (e.g., Amphilepididae) as being paedomorphic, with little explanation about how and why. It is interesting to note that the family Amphilepididae consists of only 2 genera: *Amphicutis* (with *A. stygobita* being the only species) and *Amphilepis* with about 12 species (Stöhr et al. 2024), all of which appear to be deep-sea dwellers. This may explain why the family Amphilepididae is considered paedomorphic: living in caves and the deep sea can promote paedomorphy due to evolutionary pressure to conserve energy in relatively low nutrient environments. In their study of paedomorphosis in deep-sea brittle stars, Stöhr and Martynov (2016) listed 29 morphological features they considered paedomorphic; however, they provided little explanation of why paedomorphisms occur in the deep sea, except that the paedomorphic morphology of deep-sea brittle stars “may be linked to low nutrient and energy potential of the bathyal and abyssal environments.” Here I would like to expand on this explanation for the occurrence of ophiuroid paedomorphisms in the deep sea and in *A. stygobita* in Bernier Cave.

Apparently it is well known that several cave dwelling salamander species are permanently aquatic and retain their larval gills into adulthood (i.e., paedomorphy) because they have access to a richer food source in the water than in the terrestrial cave habitat (Recknagel and Trontelj 2022). The explanation for paedomorphy in ophiuroids is much different. In most cases, paedomorphic species conserve energy by not producing, maintaining, and transporting fully developed adult body parts, and these reductions would be retained in populations if they are not disadvantageous. The survival

advantage of a specific paedomorphic trait can often be correlated with certain environmental circumstances that allow animals with juvenile traits to survive. For instance, brittle stars that are microphagous detritivores may be able to survive well with reduced mouthparts, since adults and babies can more easily consume soft detritus than passive suspension feeders that gather particulate material with their tube feet or macrophagous carnivores that grasp prey with their arms. Similarly, species with reduced arm stereoms save energy by not producing, maintaining, and transporting heavy adult ossicles if they do not need them to catch food or to survive predation or strong water flow. According to Harper and Peck (2016) there is a general paradigm that marine predation pressure decreases with depth, which they confirmed in their study of shell repair in brachiopods. In addition, ocean currents generally diminish in intensity with increasing depth (Faugères and Mulder 2011), which enables fine particles to settle out of suspension as detritus (Dutkiewics et al. 2016). Seasonal deposition of phytodetritus below productive surface areas provides abyssal communities with a high-quality food resource (Tyler 1988; Gage 2003; Ramirez-Llodra et al. 2010). Deep-sea detritus is also enriched by EPS (Thornton 2002), as it is in Bernier Cave. According to Ramirez-Llodra et al. (2010), “Much of the sediment-covered abyssal seafloor is characterized by sluggish bottom currents and little current scouring” and “the top centimetres of sediments of abyssal plains are colonized by very rich communities of macro- and meiofauna with very high biodiversity levels.” Thus, it seems likely that many deep-sea brittle star species are able to find microhabitats with slight currents, few predators, and abundant energy-rich detritus where they can survive with paedomorphic traits. More than half of the 2300 brittle star species are found in the deep sea (Stöhr et al. 2012). I contend that most of them are probably paedomorphic at least partly because of their intake of soft high-energy detritus, not by the “low nutrient and energy potential of the bathyal and abyssal environments,” as suggested by Stöhr and Martynov (2016). The cold temperatures of the deep sea may also contribute to paedomorphosis since brittle stars and their predators would have lower metabolic rates, and they would move more slowly, which could reduce chances of predation and the need for stronger stereoms.

Size appears to have a significant effect on the number and strength of certain paedomorphic traits. Stöhr and Martynov (2016) examined paedomorphic traits of 40 deep-sea species in the families Ophiuridae and Ophiolepididae which “are often quite small, with disk diameters of a few millimetres, and their skeleton consists of fewer elements than in the majority of extant species.” This could be because: (1) small species tend to be detritivores, so they can survive with reduced mouthparts, (2) they may be able to better avoid predators if they hide within the detritus, and (3) stereoms need to be stronger in larger brittle stars to support and move their heavier bodies.

Another situation in which a reduced stereom is advantageous is in swimming brittle stars. A few species are known to use swimming as a defensive escape mechanism, and a lighter body facilitates swimming (Hendler and Miller 1991). Hendler and Miller (1991) found that, “The skeletal ossicles of swimming ophiuroids are thinner and more porous than non-swimmers’ ossicles,” and the few species of “known swimming ophiuroids are deep-water species and several are widely distributed.”

Adaptations to cave environments are known as troglomorphisms, and many of these adaptations are related to ways that cave animals conserve energy in a low nutrient environment. Paedomorphisms offer an excellent way to conserve energy, both in caves (where they may be recognized as troglomorphisms) and in the deep sea; in both environments brittle stars do not need to spend energy producing adult structures that they do not need to survive. While humans generally want their offspring to grow up big and strong, in nature these traits do not always contribute to a species' survival and may even be detrimental.

Summarized here are the presumptive correlations between paedomorphisms in *A. stygobita* and its environment. The Bernier Cave environment has a remarkable set of characteristics that have provided the circumstances for *A. stygobita* to develop several sets of paedomorphic and troglomorphic traits. (1) Although most of the cave is in total darkness, the ceiling entrance is large and near the water which allows considerable detritus to enter the aquatic ecosystem. It also provides light for abundant growth of algae. These algae, in conjunction with bacteria to make EPS, help provide detritus sufficiently rich for detritivores to survive. This soft detritus can be consumed with reduced and fenestrated mouthparts. (2) The water inside Bernier Cave is hyposaline at ~14–28 ppt, which facilitates the reduced stereom of *A. stygobita* by reducing ionic precipitation. (3) The reduced water flow in this cave keeps detritus relatively stationary, which allows *A. stygobita* to reduce its ossicle weight as ballast and not get washed away. Ossicle weight is lost by greatly increasing fenestration in virtually all ossicles, including mouth and arm structures. In addition, several body parts have been reduced in size and/or changed in proportion. Most notably are the narrowed arms with strongly reduced DAPs and VAPs, reduced total arm length, but increased arm segment length (LAPs and Vs). This results in fewer arm joints, reduced arm swinging, and more podial walking (supported by enlarged podia). It also permits significant changes in structure of Vs with reduced articulation areas and muscle flanges. The LAPs and Vs have lateral extensions that hold them together while reducing weight, and (4) *A. stygobita* does not appear to have any major predators in Bernier Cave, which allows it to survive with a smaller body, reduced ossicle strength, and reduced spine number and size. The abundant detritus containing few predators should also provide a favorable environment for newly released brooded offspring, which may increase their survival rate and conserve energy for the population compared to producing many free-living larvae.

Culver (1982) mentioned that paedomorphosis “has been reported for a variety of cave organisms. For example, *Speoplatyrhinus poulsoni*, the most cave modified amblyopsid fish, shares some characters, such as body size and head size, with immature *Typhlichthys subterraneus*.” Also, Langecker and Longley (1993) found that two Texas blind catfishes exhibit “a series of apparently paedomorphic traits: a small body size, an enlarged head, a weakly ossified skeleton, and reduced muscles.” However, it appears that the significance of paedomorphisms as troglomorphisms has not been widely recognized. Although paedomorphy is not the same as troglomorphy, when paedomorphic traits occur in cave animals they should also be recognized as troglomorphisms. Perhaps it is easier to recognize paedomorphy in cave brittle stars than in many other cave animals since brittle stars do not have obvious eyes, so loss of eyes is not easily

observed in them, and other traits are more closely examined. In addition, the relationship of morphological traits to the environmental niche may not be as apparent as it is with *A. stygobita* in the unusual environment of Bernier Cave. Paedomorphisms may be more common in caves than in other habitats because the relatively stable environment and relaxed predation and competition in caves allow survival without adult structures.

Conservation of energy is a driving force in the evolution of many traits found in nature including: mammal hair and bird feathers to conserve heat energy, streamlined bodies of aquatic animals and light weight bones of birds and bats to conserve energy while moving, and paedomorphic traits of brittle stars to conserve energy of producing, maintaining, and transporting heavy adult structures. In general, paedomorphy should be a very effective way to conserve energy in a variety of animals, especially cave animals, by not having to produce and transport the many structures found in adults. Thus, it is surprising that paedomorphisms are not predominant troglomorphisms, but apparently for many species the adult structures are so valuable for protection from predators, competitors, and strong water movements that they are still produced. It seems that echinoderms may be unusual in their plasticity with many ways to produce a body that can survive in various environments.

Emson (1984) proposed the important concept of “Bone Idle.” He suggested that echinoderms are a “highly successful group in the marine environment” partly because they are the only invertebrates with an endoskeleton, which requires less energy to build and maintain than soft tissue due to its formation by ionic precipitation. Emson (1984) speculated that being “bone idle” may have been the recipe for success of echinoderms.

Even though the endoskeleton apparently gives echinoderms a competitive advantage over other invertebrates, it could still be advantageous to reduce their skeleton in certain environments. The body plan in *A. stygobita* seems to follow a modified recipe for success by having a greatly reduced endoskeleton that it uses effectively in this special cave environment with sufficient light to stimulate growth of energy-rich diatoms, few predators, and brackish water that reduces ionic precipitation.

Probable paedomorphisms and troglomorphisms in 4 cave brittle species

Since *A. stygobita* was the first known cave brittle star, Carpenter (2016) compiled a list of probable troglomorphisms that he had observed in this species, including: (1) no body pigment, (2) reduced body size, (3) elongated arm segments, (4) raised skin possibly for enhanced chemoreception, (5) muted alarm response to light, (6) reduced aggregation, (7) reduced fecundity, and (8) slow metabolism (movement and regeneration). Since SEMs show a greatly reduced density of the stereom with increased fenestration of ossicles, this trait is now added to the list (Table 1) of probable troglomorphisms for *A. stygobita*, along with other morphological features described in the above Discussion of Paedomorphisms and Troglomorphisms. Carpenter (2016) remarked in his study of *A. stygobita* that it was surprising that more brittle stars had not been found in caves, considering that brittle stars are generally photonegative, and it seemed likely that more species do live in marine caves. Three other brittle star species that are

Table 1. Probable troglomorphisms compared in four cave species. T: troglomorphism; dd: disk diameter; ND: no data.

Troglomorphism	<i>A. stygobita</i>	<i>O. cavernalis</i>	<i>O. commutabilis</i>	<i>O. xmasilluminans</i>
Body pigment	Absent (T)	Mottled/bands	Brown blotches	Creamy, bands, spots
Mouth parts	Very reduced (T)	Normal	Buccal funnel	Normal
Ossicle density	Very reduced (T)	Normal	Some reduced (T)	Normal
Disk diameter	Small, 3–4 mm (T)	Small, 5.3 mm	Normal, 11.4 mm	Small, 6.3 mm
Arm length	Short, 2.5 × dd (T)	Medium, 9 × dd	Long, 20 × dd (T)	Long, 18 × dd (T)
Arm seg. number	Reduced (~18) (T)	Normal (~75)	Many (~150) (T)	Many (~150) (T)
Arm spines	Few, short (T)	Few, short (T)	Normal	Many, long
Podia	Enlarged (T)	ND	Long, many (T)	Many (T)
Regeneration rate	Very slow (T)	ND	ND	ND

apparently cave endemics have recently been described and are compared below and in Table 1. In addition, Márques-Borrás (2020) indicated that 39 brittle star species have been reported from caves, including many that are not endemic to caves; this includes Okanishi and Fujita’s (2019) listing of 20 species of brittle stars from 8 families collected in submarine caves of the Ryukyu Islands, southwestern Japan.

Ophiozonella cavernalis. Okanishi and Fujita (2018) described two new species from specimens collected in submarine caves in Ryukyu Islands, southwestern Japan: *Ophiopsis cavitata* and *Ophiozonella cavernalis*. The authors did not claim that *O. cavitata* was a cave endemic because their “only 2 specimens were found in a single cave despite extensive searching, which suggests that this occurrence may have been random.” Also, the specimens were very similar to a non-cave specimen from northeastern Australia that was identified by Baker (1979) as *Ophiopsis rugosa* Koehler, 1898. Okanishi and Fujita (2019) later reported that 4 additional specimens of *O. cavitata* were found in another cave about 60 km from the original collection site, this time in the “entrance zone” with coral rubble, thus confirming that this species is probably not a cave endemic. However, this points out the difficulty of conclusively identifying brittle star species as cave endemics.

Okanishi and Fujita (2018) did claim that *O. cavernalis* is “an anchialine-endemic ophiuroid and the first finding from the Pacific Ocean.” They made this claim partly because “the number of *O. cavernalis* specimens is large and its presence in 4 caves suggest that it is indeed a cave endemic species with self-recruiting population.” Okanishi and Fujita (2018) said *O. cavernalis* (Amphilepidida) was found in four caves with an “anchialine environment (low salinity and water temperature).” Unfortunately, they did not indicate how low the salinity was, and they did not identify any troglomorphic traits. *Ophiozonella cavernalis* does not appear to have most of the prominent paedomorphic or troglomorphic traits seen in *A. stygobita* (e.g., reduced mouth parts, reduced stereom, and elongated arm segments), but it does have spines that are slightly reduced in size and number (3 vs. > 3 in the 31 congeners) (Okanishi and Fujita (2018)). From examining the SEM images of Okanishi and Fujita (2018), it appears that LAPs of *O. cavernalis* have substantial EPTs (extra peripheral trabeculae) that may be related to a photoreceptor system, which is described in more detail in the section below on

Ophionereis commutabilis. The lack of paedomorphic mouth structures in *O. cavernalis* may be related to the shallow habitat (8–27 m) composed of a silty-muddy bottom (Okanishi and Fujita 2018), instead of detritus. One prominent troglomorphic trait found in many cave-adapted organisms is the loss of pigment, and *O. cavernalis* has a significant color pattern described by Okanishi and Fujita (2018) as: “mottled light and dark brown on aboral disc, radial shields darker, arms variegated light brown with dark bands, a darker brown band on proximal portion of each arm spine.”

Ophionereis commutabilis Bribiesca-Contreras et al., 2019 was originally identified as an undescribed species from Mexico in the family Ophionereididae and barcoded by Bribiesca-Contreras et al. (2013). It was formally described and named in a phylogenetic paper by Bribiesca-Contreras et al. (2019). Márques-Borrás et al. (2020) meticulously compared morphologies of *O. commutabilis* to a close surface relative *Ophionereis reticulata* (Say, 1825) and determined “some characters representing potential morphological cave adaptations in *O. commutabilis*: bigger sizes, elongation of arms and tube feet and the presence of traits potentially paedomorphic.” Particularly notable was that arm lengths of *O. commutabilis* were “up to 20 times the disc diameter and a mean of 13.2 in comparison to 6.6 of *O. reticulata*.” Although Márques-Borrás et al. (2020) cited “bigger sizes” as a potential cave adaptation, their Fig. 5 indicates that both *O. commutabilis* and *O. reticulata* had exactly the same dd of 11.4 mm; but when they compared ratios of arm length/dd, *O. commutabilis* was much “bigger” (13.2 vs. 6.6) because of the greatly elongated arms of *O. commutabilis*. So, bigger size is only relevant when elongated arms are included. Feeding was not observed in this species, but the presence of elongated arms and tube feet, a well-developed buccal funnel, and a cave floor covered by soft sediments (Márques-Borrás et al. 2020) all indicate that this species is a passive suspension feeder or benthic deposit feeder.

Márques-Borrás et al. (2020) observed that the ossicles they examined with SEM were more porous in *O. commutabilis*, which they considered being potentially paedomorphic and troglomorphic; they did not mention the increased porosity as a possible way to reduce weight and conserve energy. They indicated that the salinity was 30–31 ppt where *O. commutabilis* were found, which may partly explain the more porous ossicles.

Márques-Borrás et al. (2020) made the important point that the increased porosity of dorsal arm plates (DAP) in *O. commutabilis* resulted in a partial reduction of its photoreceptor system, compared to *O. reticulata*. A brittle star photoreceptor system was first described by Hendler and Byrne (1987) for *Ophiocoma wendtii*, which (according to O’Hara et al. 2018) is now recognized as *Ophiomastix wendtii* (Müller & Troschei, 1842). This photoreceptor system included light sensitive nerve bundles below hemispheres on the outer surface of dorsal arm plates; they called these hemispheres EPTs (expanded peripheral trabeculae), which presumably concentrate light on the nerve bundles. EPTs appear in distinctive patterns in SEMs of those brittle star species that have EPTs, including *O. commutabilis* and *O. reticulata*. Márques-Borrás et al. (2020) found that “this pattern decreases the EPT density (increasing in size) on the stygobiotic specimens in comparison to its epigeal congener.” Hendler and Byrne (1987) and Hendler (2004) indicated that *Ophiocoma wendtii* has a well-developed

photoreception system, “but not every *Ophiocoma* species has a *wendtii*-type system with interactive microlens, chromatophore, and photoreceptor structures. There are species with markedly different capacities for color-change and differing lens morphology and light sensitivity among the four subgeneric groups of *Ophiocoma*.” Hendler (2004) noted that such optically efficient lenses are restricted to the relatively animated Ophiuroidea. However, Sumner-Rooney et al. (2018) were skeptical of the Hendler and Byrne (1987) photoreceptor system with microlenses, and they presented evidence that “whole-body photoreceptor networks are independent of ‘lenses’ in brittle stars.” Because EPT’s are restricted to certain groups of ophiuroids, and their potential use in photoreception in cave brittle stars has not been tested, I chose to not use their reduction or absence as a troglomorphism in comparing cave species in Table 1.

Márques-Borrás et al. (2020) did not discuss the fact that *O. commutabilis* appears to lack the common troglomorphic feature of pigmentation loss. Bribiesca-Contreras et al. (2019) described the coloration in *O. commutabilis* as “brown on the dorsal surface of the disc, with scattered large pale blotches” and “patterns were quite variable, resembling those described of other species of the genus.” Bribiesca-Contreras et al. (2019) suggested “that this diversity of colouration patterns could be a result of inhabiting a low-light environment, where pigmentation is extraneous and there might be no selective pressures for this trait.”

Ophiopsila xmasillumins Okanishi, Oba & Fujita, 2019 was described from a cave on Christmas Island, northwestern Australia. According to Okanishi et al. (2019), specimens occur on sandy bottoms with “disc buried and arms extended above the substratum.” This is consistent with passive suspension feeding behaviors described by Hendler (2018), although photos of the oral frame presented by Okanishi et al. (2019) do not clearly show a buccal funnel as illustrated by Hendler (2018) for *Ophiopsila californica* A.H. Clark, 1921, which frequently accompanies passive suspension feeding.

Arms of *O. xmasillumins* are approximately 18 times longer than disk diameter (Okanishi et al. 2019); a medium-length arm in their Fig. 2 has ~150 segments. Okanishi et al. (2019) noted that, “As suggested in previous studies of ophiuroids (Bribiesca-Contreras et al. 2013), extraordinarily long arms of species could be an adaptation to cave life.” The color is generally creamy white with yellowish bands, green bands, and yellowish spots in various locations (Okanishi et al. 2019).

Okanishi et al. (2019) also “describe bioluminescence and burying behaviour, which suggest adaptation to submarine cave environments.” Bioluminescence in *O. xmasillumins* could be useful in either attracting prey or scaring predators, including decapods and fishes that are known to inhabit this same cave (Okanishi et al. 2019). Protection from predators might also be provided by the numerous spines encircling each of the many short arm segments. Okanishi et al. (2019) observed that “other coastal congeners also show the same bioluminescence” and “it is difficult to say whether *O. xmasillumins* new species is a cave-endemic, since adequate inventory surveys around the cave have not yet been done.” Unfortunately, Okanishi et al. (2019) did not mention any probable cave adaptations for this species except for the long arms and bioluminescence, and they did not mention or make comparisons to *A. stygobita*,

O. cavernalis, or *O. commutabilis*. Although evidence for cave endemism in this species is sparse, it is still worthy of comparison to other species found in caves.

It is interesting to compare possible troglomorphisms of the three recently (2018, 2019) described species to those of *A. stygobita*. These four cave-dwelling species are greatly separated geographically and are in different taxonomic families, which indicates their troglomorphic traits evolved independently. This may partially explain why their apparent troglomorphisms vary widely. Also, since many brittle stars are photonegative and often live in dark environments, it is difficult to identify traits of cave-dwelling brittle stars as being definite troglomorphisms, rather than simply being traits of photonegative benthic animals. Table 1 compares probable troglomorphisms for the four cave species.

Troglomorphisms are often described as either regressive or constructive (Culver and Pippan 2019). The most obvious regressive traits in most cave animals are reduction in eyes and body pigment, while constructive traits include enhanced sensory structures or behaviors to help find or capture food (Culver 1982; Culver and Pippan 2019; Romero 2009). In cave brittle stars, probable regressive traits are loss or reduction in body pigment, mouth parts, ossicle density, disk diameter, arm length, arm segment number, and spine length and number; most of these regressive troglomorphic traits are also paedomorphic traits. Constructive traits in cave brittle stars may include elongated arms and enlarged or more podia to help sense and/or capture food in the substrate or suspended in the cave water; podia are larger in *A. stygobita* and more numerous in *O. commutabilis* and *O. xmasilluminaans* by virtue of their having much longer arms. On the other hand, the short arms of *A. stygobita* apparently are an advantageous paedomorphic trait because less energy is needed to produce them, and long arms are not needed to eat soft detritus. Most brittle stars have many short arm segments resulting in many podia (2 per segment) and many joints that give arm flexibility. In *A. stygobita*, energy is conserved by reducing arm segment number, which reduces total number of podia and joints; each segment is relatively long, but energy is conserved by producing fenestrated ossicles, with LAPs and Vs reinforced by lateral extensions.

Note that there is little consistency in the presence or absence of any of the troglomorphisms across the four species. Thus, it is challenging to find definite troglomorphic traits in the three ophiuroid species described after *A. stygobita* in 2011. All have pigment, and the loss of microlenses as light-detecting structures is not clear. Romero (2009) pointed out that troglomorphisms can be highly variable, blindness and depigmentation do not occur in parallel among most cave species, and “This disparity in character development among species suggest that both the evolutionary history of the species involved and the peculiar characteristics of the environment in which they live must be taken into consideration to explain such a mosaic of character development.” Several of the troglomorphic traits for *A. stygobita* described by Carpenter (2016) including a very slow regeneration rate and behavioral traits (e.g., muted alarm response to light and slow movement with podial walking) were not reported and were apparently not observed in the other three cave species; hopefully, live specimens of these three species will be studied in the future to look for such traits. Brooding, the extreme fenestration of ossicles, and elongated vertebrae with extra lateral extensions in *A. stygobita*

appear to be additional energy conserving traits. So, it appears that *A. stygobita* has more troglomorphisms and paedomorphisms than the other three species, which may be the result of a longer evolutionary history in cave habitats and/or of the special characteristics of Bernier Cave, especially low salinity and abundant detritus.

Conclusions

The cave brittle star *A. stygobita* is a small (adult dd = 3–4 mm) microphagous deposit-feeding brittle star that survived and grew in captivity by consuming detritus rich in microorganisms and a sticky biofilm containing extracellular polymeric substances (EPS). They can feed with reduced mouth parts because the detritus is soft and easy to consume. This hermaphroditic intraovarian brooding species had only ~5–7 gonads per individual with relatively large eggs and developing embryos 0.20 to 0.35 mm. Three babies born in captivity each had only two segments per arm outside the disk and produced only one additional segment per arm in about a year. The slow growth rate of babies corresponds to the very slow regeneration rate of adults.

This species has numerous paedomorphisms and troglomorphisms that appear to be related to its unusual cave habitat with reduced salinity, little tidal movement, reduced predation, and abundant detritus enriched by diatoms, EPS, and bacteria. Three other cave endemic brittle stars have much fewer troglomorphisms probably because salinity in their caves was not reduced as much, and energy-rich detritus was not available. Many deep-sea brittle star species have numerous paedomorphisms probably because some areas of the deep sea provide energy-rich detritus, along with reduced currents and predation pressure. Conservation of energy is a driving force in the evolution of many traits found in nature including reduced mouthparts and arm ossicles in brittle stars; this conserves energy by not producing, maintaining, and transporting these adult structures. Although *A. stygobita* has been found only in Bernier Cave and Lighthouse Cave and only in low numbers, it does not seem to be endangered. Few people visit Bernier Cave because it is a challenge to hike to, and the administrators at the Gerace Research Centre limit visits to protect this unusual habitat and its rare brittle stars. This species probably exists in other subterranean habitats that humans have not been able to explore. Ideally, the DNA sequence of *A. stygobita* should be analyzed for phylogenetic studies, and eDNA might be used to determine if populations of *A. stygobita* occur in other caves in the region.

Acknowledgements

I thank the Bahamian government, the Gerace Research Centre on San Salvador Island, and Executive Director Troy Dexter for logistic support and making specimens available. Special thanks to John Winter for discovering and collecting the first cave brittle stars and sending them to me; Li Newton for her many hours of cutting trails and collecting specimens; other colleagues who helped collect specimens, especially

Mark Lewin, Patty Lewin, David Cunningham, Ben Crossley, Nick Callahan, Cliff Hart, Reeda Hart, Billy Stafford, Julie Moses, and Ramamurthi Kannan; Brenda Racke for assistance with NKU's scanning electron microscope; Paula Keene Pierce of Excalibur Pathology for preparing serial sections; Chris Pomory for his excellent work on our original 2011 paper and for helpful comments on this paper; Joan Herrera and Laura Wiggins for providing preserved specimens from collections of the Florida Fish and Wildlife; Gordon Hendler for providing preserved specimens from the Natural History Museum of Los Angeles County and for sharing his extensive knowledge on brittle stars; Richard Turner for help interpreting SEM images; Miriam Closer for carefully editing the manuscript; Academic editor Fabio Stoch and Subject editor Elizabeth Borda for their encouragement and guidance during the review process; Jill Yager, Francisco Solís-Marín, and an anonymous reviewer for their valuable suggestions that improved the manuscript; and my wife Rhonda for assisting with the manuscript and for her many years of patience during this long project.

Northern Kentucky University provided financial support for my associate Julie Moses.

References

- Baker AN (1979) Some Ophiuroidea from the Tasman Sea and adjacent waters. New Zealand Journal of Zoology 6: 21–51. <https://doi.org/10.1080/03014223.1979.10428345>
- Bishop RE, Humphreys WF, Cukrov N, Žic V, Boxshall GA, Cukrov M, Iliffe TM, Kršinić F, Moore WS, Pohlman JW, Sket B (2015) “Anchialine” redefined as a subterranean estuary in a crevicular or cavernous geologic setting. Journal of Crustacean Biology 35(4): 511–514. <https://doi.org/10.1163/1937240X-00002335>
- Bribiesca-Contreras G, Solís-Marín FA, Laguarda-Figueras A, Zaldivar-Riveron A (2013) Identification of echinoderms (Echinodermata) from an anchialine cave in Cozumel Island, Mexico, using DNA barcodes. Molecular Ecology Resources 13(6): 1137–1145. <https://doi.org/10.1111/1755-0998.12098>
- Bribiesca-Contreras G, Pineda-Enríquez T, Márques-Borrás F, Solís-Marín FA, Verbruggen H, Hugall AF, O'Hara T (2019) Dark offshoot: phylogenomic data sheds light on the evolutionary history of a new species of cave brittle star. Molecular Phylogenetics and Evolution 136: 151–163. <https://doi.org/10.1016/j.ympev.2019.04.014>
- Bruckner CG, Rehm C, Grossart H, Kroth PG (2011) Growth and release of extracellular organic compounds by benthic diatoms depend on interactions with bacteria. Environmental Microbiology 13(4): 1052–1063. <https://doi.org/10.1111/j.1462-2920.2010.02411.x>
- Byrne M (1991) Reproduction, development and population biology of the Caribbean ophiuroid *Ophionereis olivacea*, a protandric hermaphrodite that broods its young. Marine Biology 111(3): 387–399. <https://doi.org/10.1007/BF01319411>
- Carpenter JH (1981) *Bahalana geracei*, n. gen., n. sp., a troglobitic marine cirolanid isopod from Lighthouse Cave, San Salvador Island, Bahamas. Bijdragen tot de Dierkunde 51(2): 259–267.
- Carpenter JH (2016) Observations on the biology and behavior of *Amphicutis stygobita*, a rare cave brittle star (Echinodermata: Ophiuroidea) from Bernier Cave, San Salvador Island,

- Bahamas. In: Erdman R, Morrison R (Eds) Proceedings of the 15th Symposium on the natural history of The Bahamas. June 2013. Gerace Research Centre, San Salvador.
- Carpenter JH (2021) Forty-year natural history study of *Bahalana geracei* Carpenter, 1981, an anchialine cave-dwelling isopod (Crustacea, Isopoda, Cirolanidae) from San Salvador Island, Bahamas: reproduction, growth, longevity, and population structure. *Subterranean Biology* 37: 105–156. <https://doi.org/10.3897/subtbiol.37.60653>
- Clark HL (1911) North Pacific ophiurans in the collection of the United States National Museum. *United States National Museum Bulletin* 75: 1–302.
- Clark HL (1917) Reports on the scientific results of the Albatross Expedition to the Tropical Pacific, 1899–1900 (Part 18). Reports on the scientific results of the Albatross Expedition to the Eastern Tropical Pacific, 1904–1905 (Part 30). Ophiuroidea. *Bulletin of the Museum of Comparative Zoology at Harvard* 61(12): 429–453.
- Clark MS, Dupont S, Rossetti H, Burns G, Thorndyke MC, Peck LS (2007) Delayed arm regeneration in the Antarctic brittle star *Ophionotus victoriae*. *Aquatic Biology* 1: 45–53. <https://doi.org/10.3354/ab00004>
- Clements LAJ, Fielman KT, Stancyk SE (1988) Regeneration by an amphiuroid brittlestar exposed to different concentrations of dissolved organic material. *Journal of Experimental Marine Biology and Ecology* 122: 47–61. [https://doi.org/10.1016/0022-0981\(88\)90211-0](https://doi.org/10.1016/0022-0981(88)90211-0)
- Culver DC (1982) *Cave Life: Evolution and Ecology*. Harvard University Press, Cambridge 189 pp. <https://doi.org/10.4159/harvard.9780674330214>
- Culver DC, Phipps T (2019) *The biology of caves and other subterranean habitats*. Oxford University Press, New York, 301 pp. <https://doi.org/10.1093/oso/9780198820765.001.0001>
- Donachy JE, Watanabe N (1986) Effects of salinity and calcium concentration on arm regeneration by *Ophiothrix angulata* (Echinodermata: Ophiuroidea). *Marine Biology* 91: 253–257. <https://doi.org/10.1007/BF00569441>
- Dutkiewicz A, Müller RD, Hogg MA, Spence P (2016) Vigorous deep-sea currents cause global anomaly in sediment accumulation in the Southern Ocean. *Geology* 44(8): 663–666. <https://doi.org/10.1130/G38143.1>
- Emson RH (1984) Bone idle – A recipe for success? *Proceedings of the Fifth International Echinoderm Conference / Galway*, 25–30. <https://doi.org/10.1201/9781003079224-5>
- Falasco E, Ector L, Isaia M, Wetzel CE, Hoffmann L, Bona F (2014) Diatom flora in subterranean ecosystems: a review. *International Journal of Speleology* 43(3): 231–251. Tampa, FL (USA) ISSN 0392-6672. <https://doi.org/10.5038/1827-806X.43.3.1>
- Faugères J, Mulder T (2011) Contour currents and contourites. In: Hüneke H, Mulder T (Eds) *Developments in deep-sea sedimentology deep-sea sediments*. Amsterdam, Elsevier: 149–214. [https://doi.org/10.1016/500-70.4571\(11\)63003-3](https://doi.org/10.1016/500-70.4571(11)63003-3)
- Gage JD (1984) On the status of the deep-sea echinoids, *Echinosigra phiale* and *E. paradoxa*. *Journal of the Marine Biological Association of the United Kingdom* 64: 157–170. <https://doi.org/10.1017/S0025315400059701>
- Gage JD (1990) Skeletal growth markers in the deep-sea brittle stars *Ophiura ljungmani* and *Ophiomusium lymani*. *Marine Biology* 104: 427–435. <https://doi.org/10.1007/BF01314346>
- Gage JD (2003) Growth and production of *Ophiocten gracilis* (Ophiuroidea: Echinodermata) on the Scottish continental slope. *Marine Biology* 143: 85–97.

- Harper EM, Peck LS (2016) Latitudinal and depth gradients in marine predation pressure. *Global Ecology and Biogeography* 25(6): 670–678. <https://doi.org/10.1111/geb.12444>
- Hendler G (1975) Adaptational significance of the patterns of ophiuroid development. *American Zoologist* 15: 691–715. <https://doi.org/10.1093/icb/15.3.691>
- Hendler G (1991) Echinodermata: Ophiuroidea. In: Gies AC, Pearse JS, Pearse VB (Eds) *Reproduction of marine invertebrates*. Vol. VI. Echinoderms and Lophophorates. Pacific Grove, California: Boxwood Press, 355–511.
- Hendler G (2004) An echinoderm's eye view of photoreception and vision. In: Heinzel T, Nebelsick JH (Eds) *Echinoderms Munchen: proceedings of the 11th international echinoderm conference*. AA Balkema Publishers, Leiden, 339–349. <https://doi.org/10.1201/9780203970881.ch56>
- Hendler G (2018) Armed to the teeth: a new paradigm for the buccal skeleton of brittle stars (Echinodermata: Ophiuroidea). *Contributions in science* 526: 189–311. <https://doi.org/10.5962/p.324539>
- Hendler G, Byrne M (1987) Fine structure of the dorsal arm plate of *Ophiocoma wendtii*: evidence for a photoreceptor system. *Zoomorphology* 107: 261–272. <https://doi.org/10.1007/BF00312172>
- Hendler G, Miller JE (1991) Swimming ophiuroids – real and imagined. *Biology of Echinodermata* (1st edn.), 179–190. <https://doi.org/10.1201/9781003077565-41>
- Hendler G, Miller JE, Pawson DL, Kier PM (1995) Sea stars, sea urchins, and allies. *Echinodermata of Florida and the Caribbean*. Smithsonian Institution Press, Washington DC, 390 pp.
- Holthuis LB (1973) Caridean shrimps found in land-locked saltwater pools at four Indo-West Pacific localities (Sinai Peninsula, Funafuti Atoll, Maui and Hawaii Islands), with the description of one new genus and four new species. *Zoologische Verhandelingen* 128: 1–48 [pls. 1–7].
- Hoskins DL, Stancyk SE, Decho AW (2003) Utilization of algal and bacterial extracellular polymeric secretions (EPS) by the deposit-feeding brittlestar *Amphipholis gracillima* (Echinodermata). *Marine Ecology Progress Series* 247: 93–101. <https://doi.org/10.3354/meps247093>
- Irimura S, Fujita T (2003) Interspecific variation of vertebral ossicle morphology in the Ophiuroidea. In: Feral JP, David B (Eds) *Echinoderm Research 2001: Proceedings of the 6th European Conference on Echinoderm Research*, Banyuls-sur-me, 3–7 September 2001, Lisse: Netherlands: AA Balkerma, 161–167.
- LaFace KMP (2019) Assessing the impact of climate-change related lower pH and lower salinity conditions on the physiology and behavior of a luminous marine invertebrate. Master of Science thesis, University of California San Diego. 86 pp.
- Langecker TG, Longley G (1993) Morphological adaptations of the Texas blind catfishes *Trogloglanis pattersoni* and *Satan eurystomus* (Siluriformes: Ictaluridae) to their underground environment. *Copeia* 1993(4): 976–686. <https://doi.org/10.2307/1447075>
- LeClair EE (1996) Arm joint articulations in the ophiuran brittlestars (Echinodermata: Ophiuroidea): a morphometric analysis of ontogenetic, serial, and interspecific variation. *Journal Zoological Society of London* 240: 245–275. <https://doi.org/10.1111/j.1469-7998.1996.th05283.x>
- Márquez-Borrás F, Solís-Marín FA, Mejía-Ortiz LM (2020) Troglomorphism in the brittle star *Ophionereis commutabilis* Bribiesca-Contreras et al., 2019 (Echinodermata,

- Ophiuroidea, Ophionereididae). *Subterranean Biology* 33: 87–108. <https://doi.org/10.3897/subtbiol.33.48721>
- O'Hara TD, Hugall AF, Thuy B, Stöhr S, Martynov AV (2017) Restructuring higher taxonomy using broad-scale phylogenomics: The living Ophiuroidea. *Molecular Phylogenetics and Evolution* 107: 415–430. <https://doi.org/10.1016/j.ympev.2016.12.006>
- O'Hara TD, Stöhr S, Hugall AF, Thuy B, Martynov A (2018) Morphological diagnoses of higher taxa in Ophiuroidea (Echinodermata) in support of a new classification. *European Journal of Taxonomy* 416: 1–35. <https://doi.org/10.5852/ejt.2018.416>
- Okanishi M, Fujita Y (2018) First finding of anchialine and submarine cave dwelling brittle stars from the Pacific Ocean, with descriptions of new species of *Ophiolepis* and *Ophiozonella* (Echinodermata: Ophiuroidea: Amphilepidida). *Zootaxa* 4377(1): 001–020. <https://doi.org/10.11646/zootaxa.4377.1.1>
- Okanishi M, Fujita Y (2019) A comprehensive taxonomic list of brittle stars (Echinodermata: Ophiuroidea) from submarine caves of the Ryukyu Islands, southwestern Japan, with a description of a rare species, *Dougaloplus echinatus* (Amphiuridae). *Zootaxa* 4571(1): 73–98. <https://doi.org/10.11646/zootaxa.4571.1.5>
- Okanishi M, Oba Y, Fujita Y (2019) Brittle stars from a submarine cave of Christmas Island, northwestern Australia, with description of a new bioluminescent species *Ophiopsila xmas-illuminans* (Echinodermata: Ophiuroidea) and notes on its behaviour. *Raffles Bulletin of Zoology* 67: 421–439. <https://doi.org/10.26107/RBZ-2019-0034>
- Pomory CM (2007) Key to the common shallow water brittle stars (Echinodermata: Ophiuroidea) of the Gulf of Mexico and Caribbean Sea. *Caribbean Journal of Science Special Publication*, 10, 42 pp. <http://caribjsci.org/epub10.pdf>
- Pomory CM, Carpenter JH, Winter JH (2011) *Amphicutis stygobita*, a new genus and new species of brittle star (Echinodermata: Ophiuroidea: Ophiurida: Amphilepididae) found in Bernier Cave, an anchialine cave on San Salvador Island, Bahamas. *Zootaxa* 3133: 50–68. <https://doi.org/10.11646/zootaxa.3133.1.3>
- Ramirez-Llodra E, Brandt A, Danovaro R, De Mol B, Escobar E, German CR, Levin LA, Martinez Arbizu P, Menot L, Buhl-Mortensen P, Narayanaswamy BE, Smith CR, Tittensor DP, Tyler PA, Vanreusel A, Vecchione M (2010) Deep, diverse and definitely different: unique attributes of the world's largest ecosystem. *Biogeosciences* 7: 2851–2899. <https://doi.org/10.5194/bg-7-2851-2010>
- Ravelo AM, Konar B, Bluhm B, Iken K (2017) Growth and reproduction of the brittle stars *Ophiura sarsii* and *Ophiocten sericeum* (Echinodermata: Ophiuroidea). *Continental Shelf Research* 139: 9–20. <https://doi.org/10.1016/j.csr.2017.03.011>
- Recknagel H, Trontelj P (2022) From cave dragons to genomics: advancements in the study of subterranean tetrapods. *Bioscience* 72(3): 254–266. <https://doi.org/10.1093/biosci/biab117>
- Roldán M, Hernández-Mariné M (2009) Exploring the secrets of the three-dimensional architecture of phototrophic biofilms in caves. *International Journal of Speleology* 38: 41–53. <https://doi.org/10.5038/1827-806X.38.1.5>
- Romero A (2009) *Cave biology, life in darkness*. Cambridge University Press, 291 pp. <https://doi.org/10.1017/CBO9780511596841>

- Ruck E, Nakov T, Alverson AJ, Theriot EC (2016a) Phylogeny, ecology, morphological evolution, and reclassification of the diatom orders Surirellales and Rhopalodiales. *Molecular Phylogenetics and Evolution* 103: 155–171. <https://doi.org/10.1016/j.ympev.2016.07.023>
- Ruck EC, Nakov T, Alverson AJ, Theriot EC (2016b) Nomenclatural transfers associated with the phylogenetic reclassification of the Surirellales and Rhopalodiales. *Notulae Algarum* 10: 1–4.
- Shnyukova EI, Zolotarova EK (2017) Ecological role of exopolysaccharides of Bacillariophyta: A review. *International Journal on Algae* 19: 5–24. <https://doi.org/10.1615/InterJAlgae.v19.i1.10>
- Sköld M, Gunnarsson SG (1996) Somatic and germinal growth of the infaunal brittle stars *Amphiura filiformis* and *A. chiajei* in response to organic enrichment. *Marine Ecology Progress Series* 142: 203–214. <https://doi.org/10.3354/meps142203>
- Steinitz-Kannan M, Carpenter JH, Nienaber MA (2025) A biofilm micro-community dominated by the diatom *Campylodiscus neofastuosus* (Surirellales) binds detritus used as food source for rare brittle stars endemic to two Bahamian caves. *Subterranean Biology* 51: 197–212. <https://doi.org/10.3897/subtbiol.51.141192>
- Stock JH, Illife TM, Williams D (1986) The concept “anchialine” reconsidered. *Stygologia* 2: 90–92.
- Stöhr S (2005) Who’s who among baby brittle stars (Echinodermata: Ophiuroidea): Postmetamorphic development of some North Atlantic forms. *Zoological Society of the Linnean Society* 143: 543–576. <https://doi.org/10.1111/j.1096-3642.2005.00155.x>
- Stöhr S, Martynov A (2016) Paedomorphosis as an evolutionary driving force: insights from deep-sea brittle stars. *PLoS ONE* 11(11): e0164562. <https://doi.org/10.1371/journal.pone.0164562>
- Stöhr S, O’Hara TD, Thuy B (2012) Global diversity of brittle stars (Echinodermata: Ophiuroidea). *PLoS ONE* 7(3): e31940. <https://doi.org/10.1371/journal.pone.0031940>
- Stöhr S, O’Hara TD, Thuy B (Eds) (2024) World Ophiuroidea Database. *Amphilepis platytata* H.L. Clark, 1911. World Register of Marine Species. <https://www.marinespecies.org/aphia.php?p=taxdetails&id=242633> [2024-03-27]
- Sumida YG, Tyler PA (1998) Postlarval development in shallow and deep-sea ophiuroids (Echinodermata: Ophiuroidea) of the NE Atlantic Ocean. *Zoological Society of the Linnean Society* 124: 267–300. <https://doi.org/10.1111/j.1096-3642.1998.tb00577.x>
- Sumner-Rooney L, Rahman IA, Sigwart JD, Ullrich-Lüter E (2018) Whole-body photoreceptor networks are independent of ‘lenses’ in brittle stars. *Proceedings Royal Society B* 285: 20172590. <https://doi.org/10.1098/rspb.2017.2590>
- Thornton D (2002) Diatom aggregation in the sea: mechanisms and ecological implications. *European Journal of Phycology* 37: 149–161. <https://doi.org/10.1017/S0967026202003657>
- Turner RL, Meyer CE (1980) Salinity tolerance of the brackish-water echinoderm *Ophiophragmus filograneus* (Ophiuroidea). *Marine Ecology Progress Series* 2: 249–256. <https://doi.org/10.3354/meps002249>
- Tyler PA (1988) Seasonality in the deep-sea. *Marine Biology* 26: 227–258.
- Webb PM, Tyler PA (1985) Post-larval development of the common north-west European brittle stars *Ophiura ophiura*, *O. albida* and *Acrocnida brachiata* (Echinodermata: Ophiuroidea). *Marine Biology* 89: 281–292. <https://doi.org/10.1007/BF00393662>